1-1-2016

Voltage Management Of Distribution Networks With High Penetration Of Distributed Photovoltaic Generation Sources

Saeed Alyami
Wayne State University,

VOLTAGE MANAGEMENT OF DISTRIBUTION NETWORKS WITH HIGH PENETRATION OF DISTRIBUTED PHOTOVOLTAIC GENERATION SOURCES

by

SAEED ALYAMI

DISSERTATION

Submitted to the Graduate School

of Wayne State University,

Detroit, Michigan

in partial fulfillment of the requirements

for the degree of

DOCTOR OF PHILOSOPHY

2016

MAJOR: ELECTRICAL ENGINEERING

Approved By:

_____

Advisor Date

_____

_____

_____

DEDICATION

To my family

ACKNOWLEDGEMENTS

First of all, it is my privilege to express my great appreciation to my advisor, Professor Caisheng Wang. I especially acknowledge him for giving me guidance, motivation, and his immense knowledge in my academic research, and improve my talents and skills. I highly appreciate his continuous support, encouragement, and patience to purse my PhD. It is my great honor to be one of his PhD students.

I would like to sincerely thank my dissertation committee Professor Le Yi Wang, Professor Feng Lin, and Dr. Jiaxin Ning who provided me valuable ideas. I greatly appreciate their suggestions that help me to improve my research study. My sincere gratitude also goes to my collaborators, Dr. Yang Wang, Junhui, and Chang Fu for their great suggestions and consultation in my PhD research. Moreover, I would like to thank my friend Zuhair for his great discussion and his valuable time during my research.

Special thanks go to my mother Fatma; I would have never forgotten her support and love. Thanks to my brothers and sisters for encouraging me to finish my PhD research. Finally, I thank my wife, Ashwaq, for her valuable time taking care about our kids and home as well.

TABLE OF CONTENTS

LIST OF TABLES

LIST OF FIGURES

CHAPTER 1 INTRODUCTION AND LITREATURE REVIEW

1.1 Motivation

Energy is very important for everyone living on this earth. In this era, people want to keep their life in better quality where they live and when they stay. With different kinds of energy, the most important need for people is electric energy, which plays vital role in quality of people's life.

The generation of the world electricity is projected to increase from 21.6 trillion kWh in 2012 by 69% to 2040, which is expected to be 36.5 trillion kWh. Based on this trend, it would reach 25.8 trillion kWh by 2020. Electricity is the fastest growing sector in the globe as it has become one of the necessary needs of the modern human society. Power systems have grown from isolated, small networks to large interconnected ones that incorporate national and international entities [1].

For decades, the electricity has been operated by using different fuels worldwide. Coal is still the major fuel used for generating the electricity but significant changes happen by using different generation fuels. Nuclear power generation was increased from 1970 till 1980, and natural gas generation grew significantly after the 1980s. In 1970s [2], the use of oil for power generation decreased because of high price, and as a result oil prices pushed power industry to search other energy sources other than oil.

In the beginning of 2000s, greenhouse gas emissions concerns pushed the environmental scientists to highlight this issue and encourage the use of renewable energy sources. Their concerns were about emissions from using oil and coal which more natural gas and a fossil fuel that emits considerably less CO2. In the International Energy outlook 2016 (IEO2016) reference case [3] generation from natural gas, nuclear, and renewable would grow up in long

term. Yet, renewable energy has been and is projected to be the fastest sector source of growing for electricity generation from 2012 till 2040 by a yearly average of 2.9% [3]. Nonhydropower renewable generation which involves wind, solar energy, PV, etc., has been estimated as a main growing source for new generation capacity in both the Organization for Economic Cooperation and Development (OECD) and non-Organization for Economic Cooperation and Development (non-OECD) regions. The estimation of nonhydropower renewables was 5% of total world power generation in 2012. Moreover, the share of nonhydropower would increase and reach 14% in 2040 according to the IEO2016 Reference case.

The second fastest growing in electricity sector after renewable energy are natural gas and nuclear power. The estimate of natural gas use from 2012 to 2040 is 2.7% each year, and electricity from nuclear power would increases by 2.4% each year. Renewable generation would generate more power than coal by 2040 as the estimation of coal generation would be at 0.8% each year [4].

Coal. Coal has the largest fuel utilized in electricity sector of power generation in the world till 2040 projection period. With the catch up of renewable generation, coal electricity generation would have surplus in 2040. Coal electricity generation, which contributed about 40% of the total world power generation in 2012, would drop to 29% in 2040 of the total world electricity generation. Although the increase of coal fired generation in 2020 to 9.7 trillion kWh from 8.6 trillion kWh in 2012, it would not go beyond 10.6 trillion kWh in 2040 [5].

China and India would become the leaders in coal fired generation, accounting by 69% of the projected worldwide; but USA has declined its production since 2008 which reached the peak of production 300 million short tons [6].

Natural gas. Natural-gas-fired power generation consumption would grow from 2012 to 2040 by 2.7% each year worldwide. Moreover, natural-gas- fired generation would increase from 22% in 2012 to 28% in 2040 of the total world electricity generation. The lower price of natural-gas-fired generation due to the contribution of shale gas as well as being more environmentally friendly keeps the increase trend of natural gas. The rate of CO2 emission of natural gas is less than the coal emission by 50%, which encourages utilities to use it for electricity generation. Furthermore, the technological efficiency of natural gas is better over generating electricity than coal.

Petroleum and other liquid fuels. According to IEO2016, petroleum and other liquid fuels are declining in the projected future by 2040 which fall from 5% in 2012 as world electricity share to a lower percent which is 2% in 2040 with 2.2% decrease in each year. Although oil has fallen to $40 per barrel this year, the oil price would rise to $140 in 2040. Thus, petroleum and other liquids continue to stay as a more expensive selective over other fuels utilized for producing electricity. The countries, which depend on using oil for generating electricity, have their own plan to decrease dependency on this fuel [5].

Nuclear power. The report of IEO2016 has mentioned the increase of generation of electricity would grow in 2012 from 2.3 trillion kWh to 4.5 kWh in 2040. Also, the share of utilization of nuclear power capacity has grown from 68% in 1980 to 80% and these factors of increasing would continue. However, under a pressure of polices in Europe and the consequences of the disaster at Fukushima Daiichi, Japan which has pushed planners to stop rely on nuclear plants, the nuclear plants would grow across the globe [5].

Renewable resources. The most dominant generation of renewable energy is still hydropower and then the other renewable sources including photovoltaic, solar energy,

geothermal, wind energy, and the other sources. Renewable energy has considered as fast growing sector in the world electricity source from the total electricity supply. The significant renewable generation increase reaches 2.9% each year and it is expected to rise from 22% to 29% in 2040 from total energy contribution. The dominant source of renewable energy is hydropower with grow of 5.7% over the other source of generation like coal, natural gas, and nuclear. However, hydropower cannot be considered as a complete sustainable way of generating electricity. The focus here is on non-hydropower renewable sources. Renewables will be interpreted as non-hydropower hereinafter. Also, renewables in general would be expected more growing than other electricity sources in United States by 2030 according to clean power plan (CPP). The expected generation of Renewables energy in 2030 is about 396 billion kWh. The fastest growing sector over renewable source is solar which has growth by 8.3% each year. The share of wind and hydroelectric power would be 33% (1.9 trillion kWh), and 859 billion kWh which about 15%[3].

There are differences between the regions of OCED and non-OECD from growth of renewable energy, which depends on average of generation increase and expected capacity for hydroelectricity according to IEO2016. OECD countries decline in their generation with regard to Non-OECD countries in nonhydropower utilization for generation of electricity by projection period in 2040. The total generation of OECD from nonhydropower is 2.3 trillion kWh (with estimate of 2.7 trillion kWh with CCP), and 2.8 trillion kWh from non-OECD on the other side. The impressive results of solar goal are mostly from contribution of India and China with other markets of countries involvement. Furthermore, the increase of solar energy for the non-OECD region is estimated by average 15.7% each year from 2012 to 2040, which

doubled the growth rates of wind energy which average of 7.7% each year and geothermal estimate of 8.6% each year[3].

1.2 Sustainable energy development

Sustainable energy has caught a special attention across the globe. With this regard, sustainable energy development is dedicated to the negotiations and discussions from different engineering aspects of sustainability in this world in order to find out an engineering approach to maintaining development from sustainable energy. The sustainability has been introduced for future development to meet the requirements of the potential enhancement in the demand of electricity. The sustainable energy development has many challenges in various aspects, including energy sources and development, efficiency evaluation, clean air and information technologies, renewable energy resources, environment capability, and alleviating of nuclear energy hazard to the environment [7] [8]. The US Department of Energy has optimistic result of decreasing the emission of CO2 in the future during the studied period from 1990 till 2040 [5].

The Brundtland Commission's Report [9] characterized the definition of sustainable energy development in 1987 into four elements which are: the increase of energy supplies to satisfy people needs for fast change in industrial countries, the decrease of the waste of conventional energy resources, and the increase in power efficiency. It also points out the health and safety concerns appearing in the utilization of energy sources. Sustainable energy development has strategies which typically include the following main technological changes: energy reserves at the end user or demand side and substituting fossil fuels by different resources of renewable energy. Accordingly, there must be plans for incorporating renewable sources in consistent energy systems subjected to energy savings and effectiveness of

efficiency [8] [10] [11].

1.2.1 World energy consumption rate

The development of economy is important stimulus source to the increase the demand of electricity. The increase of demand for electricity is going on the high rate in non-Organization for Economic Cooperation and Development (non-OECD) despite of decelerating of global gross domestic product in the former two decades according to IEO2016. Non-OECD countries reached half of generation production in 2012 of the worldwide electricity need and it would grow by 2040 to the average 61% of 22.3 trillion kWh, which higher than 11.3 trillion kWh produced in 2012.

The electric grids of OECD countries are well founded but their growth each year is less than non-OECD which consume 4.2% from their budget comparing to 2% each year from GDP of OECD countries. The net generation of OECD grows from 10.2 trillion kWh to 14.2 trillion kWh from the period of 2012 to the projection year 2040. According to the IEO2016 Reference case, the continuation of the economic growth pushes for more demand on electricity. Global GDP increases by 3.3% each year but the growing of generation increases by 1.9% each year from 2012 to 2014, which is below the economic growth [3].

1.2.2 Climate change due to energy development activities

The side effects of climate change due to influences for energy development can be classified into following elements, which are 1) altering efficiency in cooling thermal and nuclear energy production of the plants [12], 2) floods of rivers which impact the generation of power from hydro generators [13], 3) affecting agriculture production due to bioenergy [14], 4) sea change of its stream which affects the infrastructure of energy [15], 5) the effects of conditions of space weather from two sides of increasing and decreasing the temperature [16],

and finally 6) changes in space heating and cooling requirements. The causes of climate changes, which have been investigated in some research, show that demand of cooling and heating for residential areas increase the climate change due to energy consumption. The unbalance between cooling and heating with utilizing different fuels would lead to increase of yearly demand of electricity which occurs by increase cooling more than heating in each year, These situation has great impacts on climate change by using different electricity fuels [17] [18].

Climate change due to greenhouse gas (GHG) emissions has become one of the most challenging issues of modern society. To combat climate change, united efforts have been carried out worldwide to reduce GHG emissions, including the Kyoto Protocol, Copenhagen Summit, and the 2015 United Nations Climate Change Conference (UNCCC) that is to be held in Paris at the end of 2015. Although the Kyoto Protocol was not successfully implemented and there was not a workable and legal binding agreement after the Copenhagen Summit, society has been educated and awakened at an unprecedented level about the importance and seriousness of climate change issues. Moreover, many countries including the US and China are now taking realistic actions to reduce emissions production. It is also expected that "for the first time in over twenty years of United Nation negotiations, a binding and universal agreement on climate" will be achieved in the 2015 UNCCC [19].

In U.S., electric power generation contributes about 40 % of the total greenhouse gas (GHG), 64% of SO2 emissions, 16% of NOx emissions, and 68% of mercury air emissions as well as large shares of other pollutants (such as small particulates) in 2010 [20]. In contrast, most renewable energy sources produce little to no global warming emissions. As such, increasing the supply of renewable energy would significantly reduce GHG. The U.S.

Department of Energy's National Renewable Energy Laboratory explored the feasibility and environmental impacts associated with generating 80% of the country's electricity from renewable sources by 2050 and found that global warming emissions from electricity production could be reduced by approximately 81% [21].

The summit which was held in Paris, France stress to have framework for decisions and directions according to better incentives, and better methods in order to decrease the greenhouse emission. Countries agreed to reduce the greenhouse emission deforestation by using method of reservation and sustainable controlling of forest as well. The summit acknowledged that developing countries might take time to get into peaking for worldwide gas emissions, which needs more effort for accomplishing equity between emission of anthropogenic and getting rid of poverty. Moreover, the decision makers realized the significance of reducing and focusing on the consequences of greenhouse emission and recognizing the function of sustainable development change. Also, some recommendation have been addressed to the summit which each part of them should evaluate their contributions nationally each five years and show the feedback according to the Paris agreement [22].

1.3 The development of PV/solar energy system

The main utilized solar energy is solar electricity, solar fuels, and solar thermal. The major developments in electricity sector are in solar electricity, which is also called photovoltaic (PV). The research and development has been achieved to find out optimal approach for higher efficiency and lower costs [23]. PV is composed of solar cells, which have the light-absorbing materials in the layer of photoactive. The composition is established on crystalline silicon by using a p-n junction structure with doping of planar silicon (Si) to force separation of charge in order to photocurrent and photovoltage generated. The peak watt cost (one single dollar per

watt peak, $/Wp) has been decreased by 20% for cumulative module fabrication. Silicon panels, which represent 90% of solar panels in the markets by 2013, offer energy payback in less than two years with efficiency power conversion 21% [24] [25]. The decrease in panel price has come from the reduction cost of panels composition which are polymer encapsulant, silver electrical contacts, and making of Si wafer. These reductions of price would give more opportunities for producing large panel facilities. Furthermore, the research would find out some methods to increase panels' efficiency with lower cost of PV manufacturing components [24] [26].

The solar thermal is typically used in desert area such as the southwestern region of United States, Australia, Middle East and other which has high temperature [27]. The solar collector, which is mainly use to reflect the temperature, is characterized into Fresnel reflector, parabolic collector, and power towers and dish engine systems. Dish engine is mainly for producing high temperature up to 1200C [28]. The generation of electricity depends on oil or molten salt fluid and the procedure of producing electricity is heat exchange to start a turbine [29].

Solar fuel has caught attention to be used from sunlight. The liquid fuel provides 40% of global fuel demands for transportation, which used for ships, heavy trucks, and aircrafts. The solar fuel has direct and indirect production with sunlight or without sunlight. The direct process of fuel production is from sunlight to the fuel without using any form of energy in between, but a form of energy has to become the connection to produce a fuel as indirect process [30].

1.3.1 The current and future development of PV/solar energy

Solar energy is drawing more and more attentions even compared to other renewable energy sources. Firstly, solar energy is inexhaustible. Around 1.35×10^5 TW solar power can

reach the surface of the Earth and about 3.6×10^4 TW of this power is usable [31]. The total world power consumption is around 17 TW [32] less than the usable solar power. Secondly, solar energy is CO2-emission-free energy source. PV systems are defined as zero emissions or emissions-free energy systems. During PV system operations, there are zero releases of CO2, NOX, and SO2 gases and it does not contribute to global warming. As given in Table 1.1, PV systems can save 2159 pounds CO2 emission for every kWh of electricity produced by coal-fired generators.

Table 1.1 Local emission rates by plant fuel generation category year 2009 data [33].

Pollutant(lb/kWh)	Coal	Gas	Fuel Oil
NOX	2.31	0.49	24.4
SO2	8.27	0.04	2.01
CO2 equivalents	2159	903	1911

Because of the clean energy characteristic, PV has been exponentially increasing for more than two decades worldwide. For instance, the PV capacity in Germany is currently close to 40GW [34] . China is expected to deploy 70GW PVs by 2017 [35]. Now 7.9 percent electric consumption is contributed by solar power in Italy [36]. The International Energy Agency estimates that solar power will become one of the mainstream energy sources by 2050 and contribute about 11% of world electricity generation [37].

1.3.2 High penetration of Distributed PV at the distribution network

The traditional distribution systems have been designed and operated under the premise of one direction power flow from the substation source to the end users. Voltage on such feeders is typically regulated by the LTC at the substation, voltage regulators at the start of the feeders (or distributed throughout the feeders), and switched capacitor banks. The control settings of these devices are coordinated to maintain the desired voltage profile along the feeder [38].

After PVs are added to the distribution systems, the assumption that the substation is the only power source is no longer true, and the problems of voltage rise/fall and fluctuations associated with solar PVs can lead to frequent operations of voltage regulation devices. More frequent operations of these devices may in turn shorten their life cycles and increase maintenance requirements and cost.

Adjusting the load tap changer (LTC) positions of distribution transformers to regulate voltage is reported in [39], [40]. However, this approach is limited by several operational and maintenance factors [41]. Also, this approach is not effective in handling voltage rise issues that normally occur at the far ends of feeders. Reactive power compensation has been the mostly used method for voltage support at transmission level and has also been widely used in distribution networks[40], [42]. For instance, capacitor banks are often used at the distribution level for boosting voltage. To address the overvoltage issue, it may be then needed to install reactors or other VAR devices that can consume inductive reactive power. However, high penetration of PVs, which is relatively unpredictable, intermittent, consumer-owned, and nondispatchable makes current standard operations for guaranteeing power quality and not be as effective as they were in the traditional distribution systems without DGs. Many electricity utilities have to adopt conservative limits in their distribution systems if no impact assessment study is carried on [42]

1.4 The challenges introduced by High penetration of PV

The technical challenges in high penetration of PV systems include voltage problems, harmonics, grid protection, and so on, in the operation and development of modern distribution networks.

1.4.1 Voltage issues

Voltage rise and voltage variations caused by fluctuations in solar PV generation are two of the most prominent impacts of high penetrations of PV. These effects particularly happen when large amounts of solar PV are connected near the end of long and lightly loaded feeders.

The most straightforward approach is to upgrade the existing distribution network by using larger conductors and transformers [43], [42]. However, this is also the most expensive way. Due to large R/X ratios in distribution networks, the voltage profile is also highly affected by real power flow [44]. Thus, real power control is also an effective way to manage voltage profiles in distribution networks [45], [46]. Though the output powers of PVs are curtailed, if well regulated, they can still generate a certain amount of real power without causing voltage problems. Since the real power control approach does not require system upgrades or extra reactive power compensation equipment and does not increase the device ratings of PV systems, it is welcomed by utilities and customers [42]. It is worth noting that although the current IEEE 1547 standard does not allow active voltage regulation by DGs [47], including this in the new version of the standard has been discussed [48].

1.4.2 Protection

Traditional distribution system protection normally consists of a simple overcurrent protection scheme. When DGs are added to a distribution network, the current/power flows become more complicated under both normal and fault conditions due to the multiple sources in the network. It is important and necessary to analyze the impacts of DGs on the selectivity, sensitivity, and reliability of the original relay protection configuration.

Nevertheless, little effort has been carried out on the optimal placement of DGs while considering the relay protection, which is also evidenced by the comprehensive survey papers [49], [50]. A new control strategy to mitigate the impact of DGs on protection system was

studied in [51]. A methodology to determine the maximum allowable capacity of a DG taking into account voltage, loss, and protection coordination constraints was proposed in[52]. The impact of DGs capacities and positions on the line protection was analyzed in [53] and [54]. More specifically, the short circuit currents regarding the distribution networks with one, two, or three DG sources at different locations were discussed in [55] and [56]. Using the PSCAD, the impacts of DG on feeder protection with superconducting fault current limiter was analyzed in [57]. The effect of high DG penetration on protective device coordination was explored and an adaptive protection scheme as a solution to the problems identified was suggested in [58]. The type, position and the capacity of DG was discussed in [59] on how harmonic contents and protection operating times are affected by DGs.

1.4.3 Islanding

Islanding means a local area can keep energized when utility power goes down. However, this is danger for line operators who could suppose the system is disconnected. Moreover, an island could get desynchronized during the stand alone period of operation, forcing the protections to fail again and being potentially dangerous for the electronic equipment [60]. Islanding detection methods can be divided into 3 categories: passive islanding, active islanding, and remote islanding. Their pros and cons are concluded as below.

Passive islanding techniques are easy to implement due to no extra controller required, no degradation of the PV inverter power quality, and inexpensiveness. Their primary drawback is having a relatively large non-detective zone, in which an islanding detection method would fail. They also bring ineffective impact on multi-inverter systems [61] and [62]. The most commonly used passive islanding detection techniques are over/under voltage and over/under frequency [63], phase jump detection [64], monitoring harmonic [65], and monitoring change

of power output [66] and frequency [67].

Active islanding detection techniques intently inject a small disturbance at the PV inverter output for detecting island. Their main advantage is relatively smaller non-detective zone than that in passive methods. Their main drawbacks are the possibility of deteriorating output power quality that makes the PV inverter instable and complicated. The existing active techniques include impedance measurement [68], frequency shift or phase shift [69] [70].

Remote islanding detection techniques don't have non-detective zone and does not degrade the PV inverter power quality. It is also effective in multi-inverter systems. However, it is expensive to implement and has a complicated communication technique. The common communication-based techniques consist of power line carrier communication [65], signal produced by disconnect [71], supervisory control and data acquisition (SCADA) [72], and so on.

1.4.4 Harmonics and other power quality issues

Harmonic emissions from PV inverters deteriorate the power quality of the grid [73], [74]. It is crucial to be able to make accurate estimations of the power quality problems with the introduction of new PV systems [75]. Various methods are proposed regarding harmonic analysis in power systems. Among them, frequency-scanning technique is the simplest and most commonly used technique for harmonic analysis. It calculates the frequency response of a network at a particular bus or node and only requires the minimal measurements [76]. In [77], a method to find locations of major harmonic sources in distribution networks is presented, in which customer impedance is modeled using Norton equivalent circuit method. Based on the singular value decomposition (SVD), the harmonic components in a power system are statistically estimated in [78]. In [79] a neural network-based algorithm is presented that can

identify both magnitude and phase of the harmonics. Search based algorithms have been applied for the harmonic components estimation such as the Bacterial Foraging Algorithm (BFO) that is presented in [80].

1.5 Scope of studies

The main purpose of the proposed work is to solve voltage violation issues in distribution networks with integration of PVs in the distribution grid. Both the real time operations (such as controlling PV power outputs) and planning strategies (such as optimal PV placement and sizing at the design stage) will be taken into account. Meanwhile, the cost-effective of demand side management associated with smart loads such as space cooling/heating system, water heater, and clothes dryer will be also investigated. A probabilistic method will be evaluated the overvoltage risk in a distribution network with different PV capacity sizes under different load levels. All the simulations will be carried out using Matlab and Opendss software on IEEE test systems.

1.6 Structure of the dissertation

The remainder of the dissertation is organized as follows: The overvoltage and undervoltage phenomena in typical distribution networks with integration of PVs are further explained in Chapter 2. A new real power capping method is presented in Chapter 3 to prevent overvoltage by adaptively setting the power caps for PV inverters in real time. The method does not require global information and can be implemented either under a centralized supervisory control scheme or in a distributed way via consensus control. Chapter 4 studies autonomous operation schedules for three types of intelligent appliances (or residential controllable loads) without receiving external signals for cost saving and for assisting the management of possible photovoltaic generation systems installed in the same distribution

network. Chapter 5 investigates the method to mitigate overvoltage issues at the planning stage. A probabilistic method is presented in the chapter to evaluate the overvoltage risk in a distribution network with different PV capacity sizes under different load levels. Conclusion and discussions on future work are given in Chapter 6.

CHAPTER 2 VOLTAGE ISSUES OF A DISTRIBUTION NETWORK WITH HIGH PV PENETRATION

2.1 Background and Introduction

Unlike conventional power plants, wind, solar, and other renewable sources have intermittent feature because they generate electrical power relaying on the time and climatic availability of the resources. Therefore, the increase of renewable energy will bring significant technical challenges to distribution networks, such as voltage rise, protection coordination, islanding issue, harmonics, short-circuit levels, and inaccurate energy and demand metering, etc. [43], as also reviewed in Chapter 1. Traditional grids may not be able to provide satisfactory performance, especially when the penetration of renewables is higher than 20% [81],[82]. It is necessary to explore new technologies in the design, control and management of the electric grid with high penetration of PVs.

2.2 Overvoltage Issues with PV installations

As a major renewable power, the total capacity of grid-connected PV power systems in U.S. has grown exponentially from 300 MW in 2000 to about to 8.37 GW in 2014 [83]. In worldwide area, Germany has the largest PV capacity of 35.5 GW and China is the second in the rank with approximate 17 GW PVs [84]. Traditionally, when PV terminal voltage exceeds a pre-specified value, overvoltage protection in PV inverter will directly shut the PV system down that will possibly cause frequent interruptions of PV power supply, leading to significant reduction of total PV energy output, loss of customer revenue, increase of power quality problems [85-89]So, the overvoltage problem is a major focus in the prospectus.

Overvoltage phenomenon is first illustrated in the IEEE 34-node distribution network [90], as shown in Figure 2.1. Two PVs are connected to nodes 840 and 860. Overvoltage appears at

node 840 because of the reverse power flow on the feeder, shown in Figure 2.2. It is worth pointing out that in this case the PVs are installed at the nodes far away from the voltage transformer and regulator that may lead to the most serious voltage violations due to the largest voltage increase on the feeder. It is deduced that the overvoltage phenomenon can be avoided by properly placing the PVs and selecting the PV sizes.

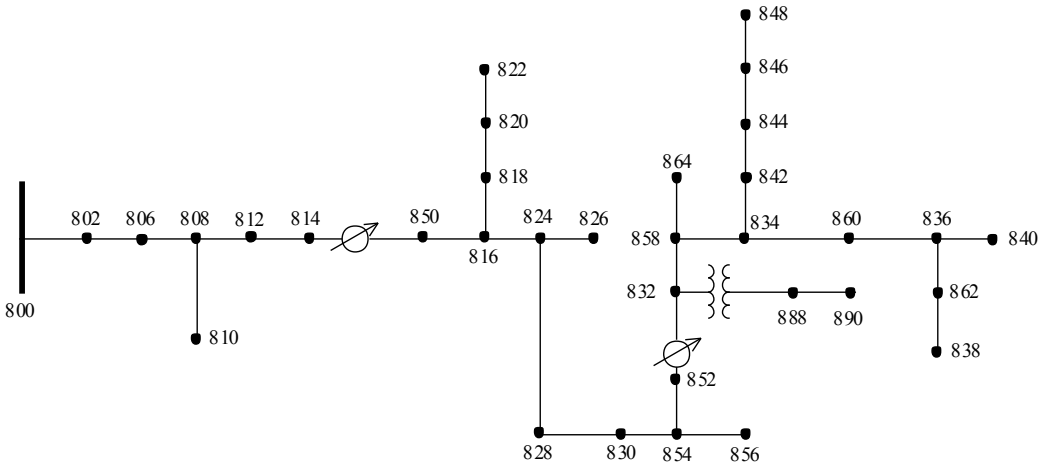

Figure 1 IEEE 34-node distribution network [91].

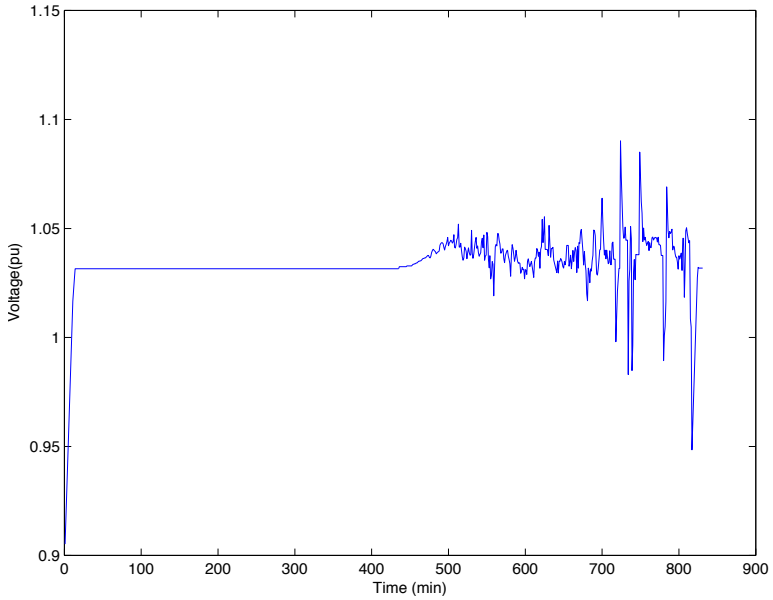

Figure 2 Overvoltage issue: Voltage profile of node 840 in the IEEE 34-node distribution network.

2.3 Undrevoltage Issues with PHEVs

Undervoltage phenomenon may also exist in distribution systems. As shown in Figure 2.1 , PHEVs are connected on whole buses except 802 with power factor of 0.894 and active power of 26.2 kW for single-phase busses and 200 kW for three phases in the IEEE 34-node system. The heavy load level happens between 4 pm and 8 pm in a day, representing a scenario that people have returned to their homes after work and been charging their PHEVs during this time period. It will lead to an overload problem in the grid while there is not sufficient or no PV power support. In Figure 2.3, the voltage at bus 814 inclines to 0.90 p.u. accordingly, which has violated the 0.95 p.u. standard [92] and may result in insufficient power output of motors and even trig undervoltage load shedding events.

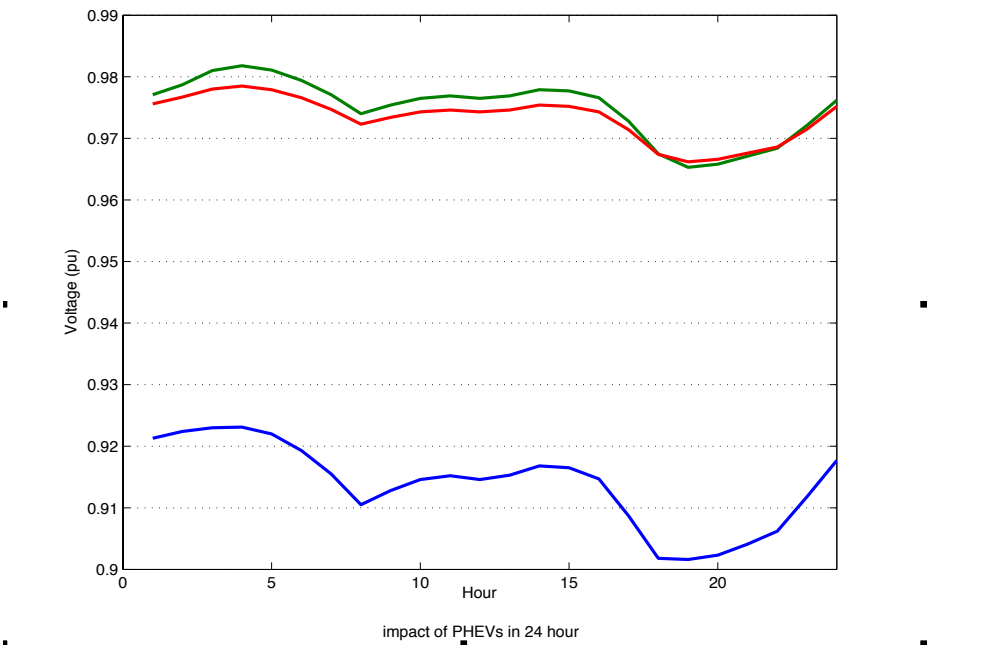

Figure 3 Undervoltage Issue: Voltage profile of node 814 in the IEEE 34-node distribution network.

2.4 Load Management

Demand-side mangament (DSM) is a set of programs that allow customers shifting their own eletricity demand during peak hours and reducing overall energy consumption. DSM could be benefitial not only to the customers who select to share actively in electricity markets, but would also assist utilities to reduce cost in energy procurement and postpone generation and tranmssion line installations to get the biggest profits. DSM usually includes energy efficiency and demand response (DR) such as turning on/off lighting, air conditioning, pumps, and other non-essential equipment in terms of the price incentives. We will also investigate the impact of PHEVs on demand response programs or markets by switching betweem charging and dischanging statuses, thereby reducing demand and cost on the grid.

2.4.1 Plug in Hybrid Electric Vehicles (PHEVs)

Plug-in hybrid electric vehicle (PHEVs) have great potentials in serving the electric grid as independent distributed energy sources. They can remain connected to grid and be ready to

deliver the energy stored in their batteries under the concept of vehicle to grid (V2G) [93]. The peak load shifting strategy using PHEVs can decrease on-peak load demand and energy consumption, which in turn will decrease the electricity buy cost for the consumer and vehicle owner [94]. PHEVs can also participate in ancillary service markets as a means of generating additional profits [95]. However, uncontrolled and random PHEV charging can produce boosted power losses, overloads and voltage fluctuations, which are all detrimental to the reliability and security of newly developing distribution networks [96]. Meanwhile, the operations of the coordinated charging is not without costs [97]. A study on the effect of different electricity and gas purchase prices on optimal PHEV power management support the effectiveness of the cost reduction [98].

On the other hand, intelligent scheduling of PHEV charging requires advanced metering, information and communication, and control systems. Meanwhile, the real-time the characteristic parameters (i.e. driving patterns, state of charge, total capacity, etc.) of the aggregated PHEVs for the network management response could be also needed in DSM. This is shifting the existing grid to the future electric grid network where the smart metering and advanced information and communication technology (ICT) [95] should be adopted.

2.4.2 Appliances Management

Controllable loads are the loads that can be controlled without noticeable effect on the customer's life manner. Loads in this type can involve space cooling, space heating, water heater, and clothes dryer loads [99]. As the details about appliances' operation are completely transparent to the grid, only limited information exchange is needed between the consumers and the suppliers. The proposed system structure in [100] enables hierarchical control, allowing to cope with more elaborate objectives related to energy management in the smart

grid, including long-term performance optimization, integration of renewable energy sources, stability enhancement, and energy trading. It is likely that a demand response event could generate a high off-peak demand due to load contributions. This proves that there is a limit on how much demand response can be acheived [101]. The appliances operations schedule can be utilized in home/building energy-management systems to help household owners or building managers to automatically generate optimal load operation schedules based on different cost and comfort settings and compare cost/benefits [102]. Global objectives like peak paving or forming a virtual power plant can be accomplished without affecting the comfort of people [103]. The the virtual power plant (VPP) concept, which consists of accumalating the capability of many distributed energy resources (DER) is able to obtain the highest load reduction over a considered control period by obtaining the optimal control strategies to be applied to a group of controllable customers [104].

CHAPTER 3 ADAPTIVE REAL POWER CAPPING METHOD FOR FAIR OVERVOLTAGE REGULATION OF DISTRIBUTION NETWORKS WITH HIGH PENETRATION OF PV

3.1 Overview

The high penetration of PV systems and other DG sources has led to great technical challenges and concerns over distribution network operations [105], [106]. Overvoltage is one of the most significant of these concerns since it is not only a power quality issue but also a problem that can decrease system reliability and the utilization level of PV systems. If not well managed, overvoltage can cause PV systems to be tripped off, affecting both power delivery reliability and the PV owners' revenue [107-109].

Various approaches have been proposed to address the voltage rise issue due to high penetration of PV systems. The most straightforward approach is to upgrade the existing distribution network by using larger conductors and transformers [109], [110]. However, this is also the most expensive way. Adjusting the load tap changer (LTC) positions of distribution transformers to regulate voltage is another way to maintain voltage profile [111, 112]. However, this approach is limited by several operational and maintenance factors [113]. Also, this approach is not effective in handling voltage rise issues that normally occur at the far ends of feeders. Reactive power compensation has been the mostly used method for voltage support at transmission level and has also been widely used in distribution networks [110, 112]. Capacitor banks are often used at the distribution level for boosting voltage. To provide reactive power compensation to address the overvoltage issue, it may be then needed to install reactors, other VAR devices that can consume inductive reactive power, or require DG sources to provide reactive power support. None of the above approaches is economically favored by utilities or customers.

Due to large R/X ratios in distribution networks, the voltage profile is also highly affected by real power flow [44]. Thus, real power control is also an effective way to manage voltage profiles in distribution networks [45], [114]. Though the output powers of PVs are curtailed, if well regulated, they can still generate a certain amount of real power without causing voltage problems. Since the real power control approach does not require system upgrades or extra reactive power compensation equipment and does not increase the device ratings of PV systems, it is welcomed by utilities and customers [110]. It is worth noting that although the current IEEE 1547 standard does not allow active voltage regulation by DGs [115], including this in the new version of the standard has been discussed [48].

A number of real power regulation methods have been proposed to address overvoltage issues due to high PV penetration. Energy storage is an effective way to accommodate intermittent PV sources and to help manage voltage profile [116]. However, the high cost of energy storage units impedes the wide use of this method. Active power droop control (voltage versus power) is used for voltage regulation in distribution networks (or microgrids) when the R/X ratios of feeders are normally high [44, 110]. Interesting studies were carried out using sensitivity methods to regulate voltage [117], [118]. Sensitivity methods, however, require full information on the entire system in order to calculate the Jacobian matrix for V-Q and V-P sensitivities. A Thevenin equivalent based real power control method was given in [109] for PV overvoltage prevention by finding dynamic Thevenin equivalent circuits from the points of common coupling (PCC) of PVs. However, the effectiveness of the method can be significantly impacted by the accuracy of equivalent circuits.

It is also important to guarantee customer fair participation and shared responsibility. For example, it is desirable to give different PVs that may be owned by different owners equal

opportunity to generate power, and to share the responsibility when PV output powers need to be regulated. This unique characteristic of fairness of power management in distribution networks has been realized by researchers recently [110, 119, 120]. An adaptive droop-based active power curtailment technique was proposed in [110] to fairly reduce the PV output powers of 12 houses along a hypothetical 240-V/75 kVA Canadian distribution feeder. However, like other voltage sensitivity analysis based methods, this technique needs the global information to compute the voltage sensitivity matrix.

This chapter proposes a new real power capping method to regulate voltage profiles of distribution networks with high penetration of PVs. By adaptively setting the power caps for PV inverters in real time, the proposed method can maintain the voltage profile within the pre-set limit while maximizing the PV generation and fairly distributing the real power curtailments among the PVs in the system. The method does not require global information and can be implemented either in a centralized supervisory control scheme or in a distributed way via consensus control. Various simulation studies have been carried out on a 33-bus distribution system and the IEEE 13-bus feeder to verify the effectiveness of the method.

The remainder of this chapter is organized as follow: Section 3.2 presents the adaptive real power capping method to control the output powers of PV systems for voltage regulation. Section 3.3 addresses the fair sharing of power curtailment among different PV systems. Steady state and dynamic simulation studies and results on the two IEEE test systems are given in Section 3.4 to verify the proposed method in different scenarios. The conclusion is given in Section 3.5.

3.2 REAL Power Capping Control

To guarantee power quality and operational security, the normal operating voltage of a grid-connected PV system falls into a narrow range that is determined by international standards, national codes and/or utility practice guidelines. For example, in the U.S.A, the normal operating range of a PV system is typically set to be 0.95 – 1.05 p.u. [121, 122] while it is 0.917 -1.042 p.u in Canada [123, 124]. Under extreme conditions, the lower and upper bounds can be loosened to be 0.88 - 1.1 p.u. [121, 122] in the U.S.A and 0.88 p.u. – 1.058 p.u. in Canada [123, 124]. When the voltage is beyond the operating condition range, the PV system needs to be cut off in a very short period of time, i.e. from a few cycles to a couple of seconds [122]. Without loss of generality, in this work, the overvoltage thresholds of alarm/warning and action are set to be 1.042 p.u. and 1.058 p.u., also called $V_{c,1}$ and $V_{c,2}$, respectively.

If the voltage of bus k (v_k) with PV installed reaches $V_{c,1}$ at time t_0, the PV controller/inverter at the bus will send out an alarm signal to notify all the other PVs in the system to start recording their power outputs and bus voltages, i.e., $p_j(t_0),\ v_j(t_0), j = 1, \cdots, r$, where r is the total number of the buses with PV installed. Bus k is called the critical bus at the moment. If the voltage of the critical bus (i.e., bus k) continues increasing, the real power capping control is activated to prevent the PV terminal voltage from going over $V_{c,2}$.

In reality, PV controllers/inverters perform at discrete steps, such as 0.5% p.u. of voltage change or a fixed time step. When the voltage at bus k reaches $(V_{c,1} + 0.5\%)$ at time t_1, for example, the controller at bus k will broadcast another message to all the other PV controllers and ask them to record their corresponding new PV outputs and bus voltages, i.e., $p_j(t_1)$, $v_j(t_1), j = 1, \cdots, r$. Based on the power and voltage records at the two different time points, a

real power capping control method is developed in this chapter to predict the power caps for the PV generator at bus k and the other PV generators. The power curtailment of a PV can be obtained by comparing its power cap value and the maximum power that it can generate based on the maximum power point tracking (MPPT) calculation. The power caps for all the PV buses will be adaptively updated at every step. The whole process is called the real power CApping Control (CAC). The details of the proposed method are given in the remainder of this section.

3.2.1 Real Power Capping Control for the Critical Bus.

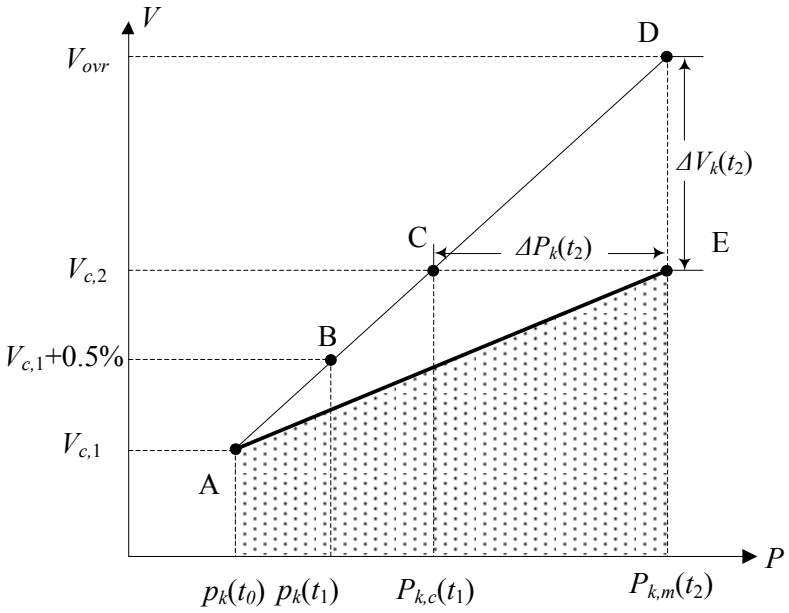

Figure 4 PV power capping control for voltage regulation: At bus k.

As shown in Figure 3.2 , point A is the condition when the voltage of bus k reaches $V_{c,1}$ at time t_0. The corresponding PV injection power is $p_k(t_0)$. Without loss of generality, suppose at time t_1 the voltage of bus k (v_k) reaches ($V_{c,1}$ + 0.5% p.u.) while its output power is $p_k(t_1)$. The slope of line AB can be calculated as

$$\rho_k^1 = \frac{v_k(t_1) - v_k(t_0)}{p_k(t_1) - p_k(t_0)} \quad (3.1)$$

The small change in voltage is approximated to be linear with the power variation in the small time span (t_0 - t_1). This is a reasonable approximation that will be validated by the simulation results given in Section IV. Extend line AB to point C where the line crosses the horizontal voltage line of $V_{c,2}$. The corresponding power $P_{k,c}(t_1)$ is the power cap of the PV at bus k which can be predicted based on the data available at time t_0 and t_1. $P_{k,c}(t_1)$ is calculated as

$$P_{k,c}(t_1) = p_k(t_0) + (V_{c,2} - V_{c,1})/\rho_k^1 \quad (3.2)$$

If the PV output power changes to $P_{k,m}(t_2)$ at the next time point t_2 due to the variation of solar insolation, to prevent unexpected overvoltage, the reference power of PV inverter at bus k can be set to

$$P_{ref,k}(t_2) = \min\left(P_{k,c}(t_1), P_{k,m}(t_2)\right) \quad (3.3)$$

where $P_{k,c}(t_1)$ is the power cap that is forecasted at time t_1 and $P_{k,m}(t_2)$ is the maximum PV output power at time t_2 based on the MPPT control. Obviously, the PV system will output $P_{k,m}(t_2)$ (i.e., the power based on the MPPT) if $P_{k,c}(t_1)$ is greater than $P_{k,m}(t_2)$. On the other hand, if $P_{k,c}(t_1) < P_{k,m}(t_2)$, the PV power will be curtailed and the power curtailment can be calculated as

$$\Delta P_k(t_2) = P_{k,m}(t_2) - P_{ref,k}(t_2) = P_{k,m}(t_2) - P_{k,c}(t_1) \quad (3.4)$$

$P_{ref,k}$ will be updated at each step based on the most recent data. The corresponding amount of power curtailment if any also changes at each step adaptively.

Note that in the figure, point D indicates the possible overvoltage if we do not take any action to constrain the PV's output; correspondingly, $\Delta V_k(t_2)$ is the voltage difference over the extreme voltage $V_{c,2}$.

3.2.2 Power Capping Regulation for the Other Photovoltaic Buses.

In fact, the voltage at bus *k* is not only dependent on the PV output at bus *k*, but also on the outputs of all the other PVs, which need to be controlled as well for voltage regulation. The following is the calculation of the power caps for all the other PV buses (e.g. bus $j \neq k$) in the network.

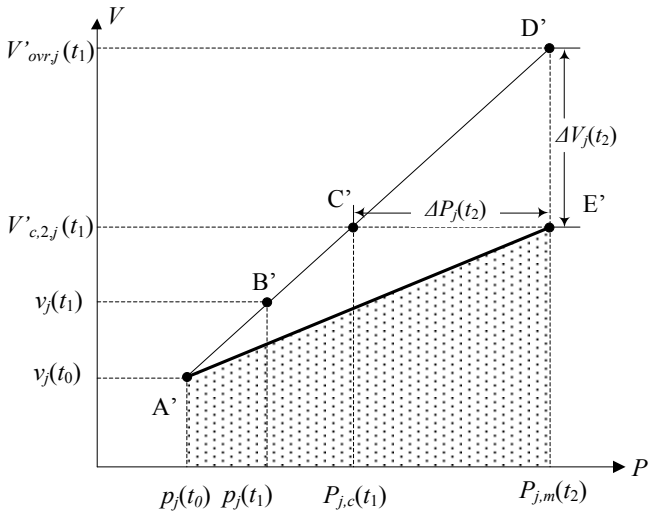

Figure 5 PV power capping control for voltage regulation: At bus *j*.

As shown in Figure 3.2, for bus *j*, point A' corresponds to point A in Figure 3.1 when the voltage of bus *k* (the critical bus) reaches $V_{c,1}$ at time t_0 (see Figure 3.1). Point B' is the operating point of bus *j* at time t_1. Accordingly, the slope of line A'B' is

$$\rho_j^1 = \frac{v_j(t_1) - v_j(t_0)}{p_j(t_1) - p_j(t_0)} \tag{3.5}$$

Similar to the process of the treatment of bus k, the critical voltage of bus j ($V'_{c,2,j}(t_1)$) for power capping can be estimated as

$$\frac{V_{c,2}-v_k(t_1)}{v_k(t_1)-V_{c,1}} = \frac{V'_{c,2,j}(t_1)-v_j(t_1)}{v_j(t_1)-v_j(t_0)} \tag{3.6}$$

and

$$V'_{c,2,j}(t_1) = v_j(t_1) + \frac{V_{c,2}-v_k(t_1)}{v_k(t_1)-V_{c,1}} \cdot \left[v_j(t_1) - v_j(t_0)\right] \tag{3.7}$$

In terms of the slope of line A'B' in (3.5), the power cap $P_{j,c}(t_1)$ of bus j at time t_1 can be calculated as

$$P_{j,c}(t_1) = p_j(t_0) + (V'_{c,2,j}(t_1) - v_j(t_0))/\rho_j^1 \tag{3.8}$$

The reference power for the PV inverter at bus j can be set to

$$P_{ref,j}(t_2) = \min\left(P_{j,c}(t_1), P_{j,m}(t_2)\right) \tag{3.9}$$

where $P_{j,m}(t_2)$ is the maximum power that PV j can generate based on the MPPT. The active power curtailed if any can be calculated as

$$\Delta P_j(t_2) = P_{j,m}(t_2) - P_{ref,j}(t_1) \tag{3.10}$$

Note that $P_{ref,j}(t_1)$ will also be updated based on the most recent data.

Similar to point D in Figure 3.1, point D' in Figure 3.2 is the possible overvoltage at bus j if no power reduction is taken at bus j; $\Delta V_j(t_2)$ would then be the voltage difference over the voltage $V'_{c,2,j}(t_1)$.

3.3 Fair Sharing of Power Curtailment

It is important for all the distributed PVs in a distribution network (or a Microgrid) to be treated in a fair way for equal customer participation. It can be readily shown that if all the PVs in a distribution network are under the same varying solar irradiance (i.e. a uniform solar

irradiance in the distribution network), the proposed power capping scheme is also a fair sharing method of power curtailment. In other words, under uniform solar irradiances, by implementing the local controls given in (3.4) and (3.10), the fair power curtailments of (3.11), discussed below, are automatically achieved. Therefore, in this section, the discussion on fair sharing of power curtailment is for the cases when the solar irradiances are diverse over the network. In the following, two approaches (centralized and distributed) to the fair sharing of PV power curtailment are discussed.

3.3.1 Centralized Control

Based on the power capping method, the fair reduction (ΔP_i^*) for each PV generator can be calculated as

$$\Delta P_i^*(t) = \frac{\sum_{j=1}^{r} \Delta P_j(t)}{\sum_{j=1}^{r} P_{j,m}(t)} P_{i,m}(t) \qquad (3.11)$$

where ΔP_j is the power curtailment at bus j calculated by the power capping method (see (3.4) or (3.10)); $P_{i,m}$ (or $P_{j,m}$) denotes the maximum output the PV at bus i (or bus j) might generate according to MPPT.

If there exists an area control center to monitor and manage all the PV voltages and power outputs, it is then straightforward to calculate the fair reduction ΔP_i^* for each bus based on (3.11) at the control center. ΔP_i^* will then be sent back to each PV generator to set its new power reference.

3.3.2 Consensus Control

If there is no area central controller (or there is a problem with the central controller), and/or if only limited communication links are available between PVs, the weighted consensus

control proposed in [125, 126] can be used to still achieve a fair power curtailment among the PVs in a distributed way.

Consensus control (COC), an emerging field in networked control [126-129], is a distributed control strategy to achieve global coordination of all subsystems. The weighted consensus control methodology in [125, 126] is uniquely suitable for our method because 1) the total amount of power reduction has been attained in advance before taking the consensus control, and it will remain unchanged in the process of consensus control; and 2) the adaptive power capping method can provide a good initial position for the consensus control, which will effectively shorten the number of iterations and computation time.

The consensus control method is carried out at discrete-time steps. At control step n, the PV power curtailment vector is denoted by $\Delta \boldsymbol{P}^n = [\Delta p_1^n, \dots, \Delta p_i^n, \dots, \Delta p_r^n]$ and $\sum_{i=1}^{r} \Delta p_i^n$ is kept constant during the process, i.e. $\sum_{i=1}^{r} \Delta p_i^n = \cdots = \sum_{i=1}^{r} \Delta p_i^1 = \sum_{i=1}^{r} \Delta P_i$. Note that ΔP_i represents the real power curtailment of bus i, which is obtained using the power capping control method. Without loss of generality, the updated power reduction at n+1 step for bus i is

$$\Delta p_i^{n+1} = \Delta p_i^n + u_i^n \tag{3.12}$$

According to (3.12), the problem becomes how to calculate the updated value u_i^n. In our method, it is assumed that each PV generator only receives information from its neighbors. Two PV generators are defined as neighbors to each other when there are one or more communication links between them. Then u_i^n can be described by the link control signal δ_{ij}^n, i.e.,

$$u_i^n = -\sum_{(i,j)\in G} \delta_{ij}^n + \sum_{(j,i)\in G} \delta_{ji}^n \tag{3.13}$$

where G is the set of links in the system; link (i, j) denotes the information flow on the link is from bus i to bus j, so is link (j, i); The link control signal δ_{ij}^n, which reflects the difference between the power curtailments at the terminal buses of link (i, j), is defined by

$$\delta_{ij}^n = \frac{\Delta p_i^n}{\gamma_i} - \frac{\Delta p_j^n}{\gamma_j} \tag{3.14}$$

where γ_i and γ_j are the weighting factors that can be determined from actual applications for the PVs at bus i and bus j, respectively. In this work, γ_i and γ_j are chosen as $P_{i,m}$ and $P_{j,m}$, i.e., the MPPT power of the PVs at buses i and j, respectively.

The above equations (3.12)-(3.14) can be written in matrix form:

$$\boldsymbol{\delta}^n = \boldsymbol{H}_2 \boldsymbol{\psi} \Delta \boldsymbol{P}^n - \widetilde{\boldsymbol{\psi}} \boldsymbol{H}_1 \Delta \boldsymbol{P}^n = \boldsymbol{H} \Delta \boldsymbol{P}^n, \text{ and} \tag{3.15}$$

$$\boldsymbol{u}^n = -(\boldsymbol{H}_2 - \boldsymbol{H}_1)^T \boldsymbol{H} \Delta \boldsymbol{P}^n \tag{3.16}$$

where $\boldsymbol{H}_1$ is a $l \times r$ matrix whose rows are elementary vectors such that if the kth link in G is link (i, j) then the kth row in $\boldsymbol{H}_1$ is a row vector with all zeros except for a "1" at the jth position. l is the total number of communication links and r is the total number of buses with PV installed. $\boldsymbol{H}_2$ is also a $l \times r$ matrix whose row are elementary vectors such that if the kth link G is link (i, j) then the kth row in $\boldsymbol{H}_2$ is the row vector of all zeros except for a "1" at the ith position. $\boldsymbol{\psi}$ is a $r \times r$ diagonal matrix whose ith diagonal elements is $1/\gamma_i$. $\widetilde{\boldsymbol{\psi}}$ is an $l \times l$ diagonal matrix whose kth diagonal elements is $1/\gamma_j$ if the kth link in the link set G is (i, j). The superscript T is the symbol of matrix transpose.

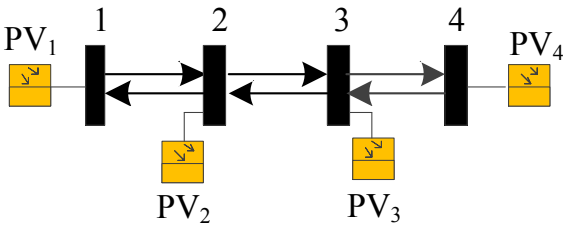

Figure 6. Communication network for a 4-PV system.

For example, for a 4-PV system in Figure 3.3, if the communication link set is $G = \{(1,2),(2,1),(2,3),(3,2),(3,4),(4,3)\}$ as shown in Figure 3.3, then the $\boldsymbol{H}_1$ and $\boldsymbol{H}_2$ are expressed as

$$\boldsymbol{H}_1 = \begin{bmatrix} 0&1&0&0 \\ 1&0&0&0 \\ 0&0&1&0 \\ 0&1&0&0 \\ 0&0&0&1 \\ 0&0&1&0 \end{bmatrix}, \text{ and } \boldsymbol{H}_2 = \begin{bmatrix} 1&0&0&0 \\ 0&1&0&0 \\ 0&1&0&0 \\ 0&0&1&0 \\ 0&0&1&0 \\ 0&0&0&1 \end{bmatrix}$$

If the weighting factors $\boldsymbol{\gamma} = [12, 15, 20, 28]^T$, we have

$$\boldsymbol{\psi} = diag\left[\frac{1}{12}, \frac{1}{15}, \frac{1}{20}, \frac{1}{28}\right], \text{and}$$

$$\widetilde{\boldsymbol{\psi}} = diag\left[\frac{1}{15}, \frac{1}{12}, \frac{1}{20}, \frac{1}{15}, \frac{1}{28}, \frac{1}{20}\right]$$

As such, the matrix $\boldsymbol{H}$ is

$$\boldsymbol{H} = \boldsymbol{H}_2\,\boldsymbol{\psi} - \widetilde{\boldsymbol{\psi}}\boldsymbol{H}_1 = \begin{bmatrix} 1/12 & -1/15 & 0 & 0 \\ -1/12 & 1/15 & 0 & 0 \\ 0 & 1/15 & -1/20 & 0 \\ 0 & -1/15 & 1/20 & 0 \\ 0 & 0 & 1/20 & -1/28 \\ 0 & 0 & -1/20 & 1/28 \end{bmatrix}$$

Substituting $\boldsymbol{H}, \boldsymbol{H}_1$ and $\boldsymbol{H}_2$ to (16) yields the updated values u_1^n~u_4^n, i.e.,

$$\begin{bmatrix} u_1^n \\ u_2^n \\ u_3^n \\ u_4^n \end{bmatrix} = \begin{bmatrix} -1/6 & 2/15 & 0 & 0 \\ 1/6 & -4/15 & 1/10 & 0 \\ 0 & 2/15 & -1/5 & 1/14 \\ 0 & 0 & 1/10 & -1/14 \end{bmatrix} \begin{bmatrix} \Delta p_1^n \\ \Delta p_2^n \\ \Delta p_3^n \\ \Delta p_4^n \end{bmatrix}$$

where Δp_1^n - Δp_4^n represent the power curtailments at step n.

It has been proven in [125, 126] that the update process can converge to the consensus weighted power, namely

$$\frac{\Delta p_i(t)}{\gamma_i} \to \beta \tag{3.17}$$

where β is a constant and equals

$$\beta = \frac{\sum_{i=1}^{r} \Delta P_i}{\gamma_1 + \cdots + \gamma_r} \tag{3.18}$$

Let $\mathbb{I}$ and $\mathbf{0}$ represent two l-dimensional column vectors with all "1" elements and all "0" elements respectively, it can be directly verified that $\tilde{\boldsymbol{\psi}}\boldsymbol{H}_1\boldsymbol{\psi}^{-1} = \boldsymbol{H}_1$, $\boldsymbol{H}\boldsymbol{\psi}^{-1}\mathbb{I} = (\boldsymbol{H}_2 - \boldsymbol{H}_1)\mathbb{I} = \mathbf{0}$ and $\psi^{-1}\mathbb{I} = \gamma$. These imply

$$\mathbb{I}^T\boldsymbol{u}^n = \mathbb{I}^T(\boldsymbol{H}_2 - \boldsymbol{H}_1)^T\boldsymbol{H}\Delta\boldsymbol{P}^n = \mathbf{0} \qquad (3.19)$$

The sum of the updated values always equals zero. Therefore, our method can assure the total amount of power reduction remains unchanged at each updated step in the consensus control, i.e.

$$\sum_{i=1}^{r}\Delta P_i = \sum_{i=1}^{r}\Delta p_i^1 = \cdots \sum_{i=1}^{r}\Delta p_i^n = \sum_{i=1}^{r}\Delta p_i^{n+1} \quad ...(3.20)$$

3.4 Case Studies

The advantages of the proposed power capping and consensus control method lie in 1) the method relies on the local voltage and power measurements and does not require global system information such as the whole system operating conditions, the network topology and line parameters that are subject to change and may be difficult to obtain. 2) By adaptively setting the power caps for all the PV generators, the method coordinates the actions of all the PVs at different buses to achieve the voltage regulation goal. 3) The fair sharing control of power curtailment for all the PVs in the system can be done either in a centralized way or a distributed way via consensus control. In order to validate the effectiveness of the power capping method with fair sharing control, case studies have been carried out for different scenarios on a 33-bus system and the IEEE 13-bus test feeder using real measured solar irradiance data and a practical load profile.

3.4.1 33-Bus System

The proposed overvoltage control methods are first verified on a 33-bus system, shown in Figure 3.4 [130]. The system has a peak load of 4.2 MW real power and 3 MVar reactive power, as well as a total of 5.95 MW (peak) PVs (10×0.15MW PVs on buses 1-10, 10×0.175MW PVs on buses 11-20, and 12×0.225MW PVs on buses 21-32). A transformer with a LTC is added to the original system. The voltage of bus 0 is regulated to be 1.04 p.u. by the LTC in the simulation studies. Three typical solar irradiance (SI) curves in Figure 3.5 are used for the 32 PVs in the simulations. The SI data were recently measured by a Davis Vantage Pro 2 weather station installed for an 8.3 kW hybrid Wind/PV system at Wayne State University, Michigan, USA The daily load profile in the system is shown in Figure 3.6, which reflects the load of a typical mid-size community in southern Michigan. Here, uniform solar irradiance in the whole system and diverse irradiances at various groups of buses are investigated. The simulation results are given and discussed in the following.

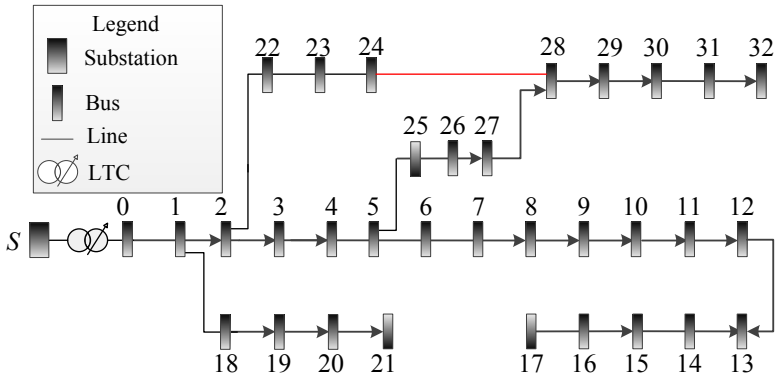

Figure 7. A 33-bus test system [130].

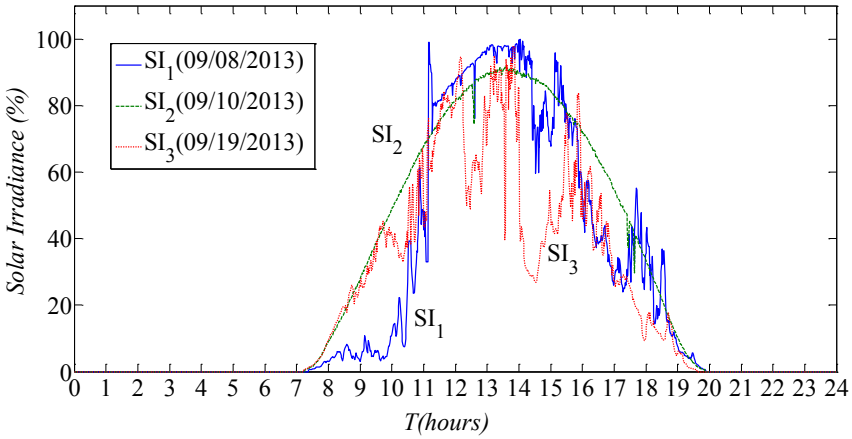

Figure 8. Three typical solar irrandiance curves.

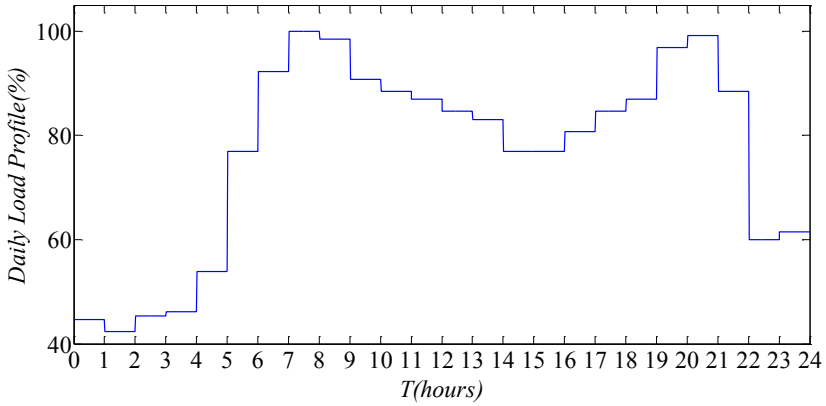

Figure 9. Daily load profile of a mid-size community in southern Michigan - served by Detroit Edison.

3.4.1.1 Uniform solar irradiance

In this case, each of the solar irradiance curves in Figure 3.5 is used for all the PVs in the 33-bus system. The 24-hour voltage profiles of bus 32 that has the highest voltage in the system are shown in Figures 3.7 (a) – (c). Each figure corresponds to a typical SI curve in Figure 3.5. If there is no capping control (NC), overvoltage will occur at several buses including bus 32. As a result, the PVs at those buses will be disconnected from the system when their voltages go over the threshold action value, i.e., 1.058 p.u. in this work. But, when the proposed power capping control (CAC) is applied, all the bus voltages are regulated to stay below or very close to the predefined upper bound, i.e., 1.058 p.u., without triggering the

overvoltage protection. This implies that the CAC method is effective when all the PVs in the same area share the same solar irradiance.

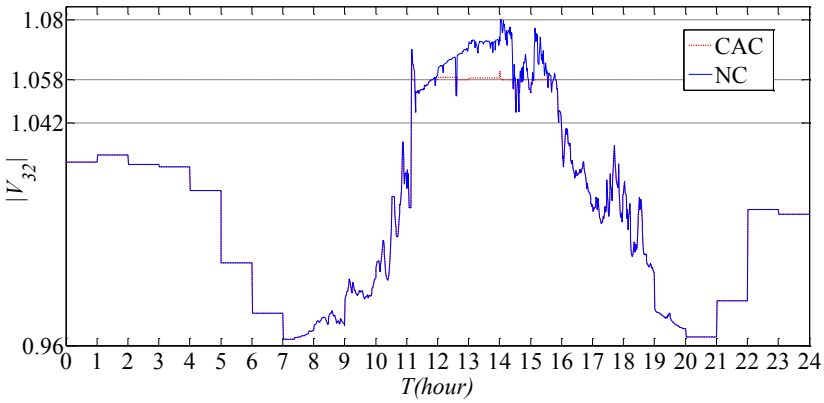

(a) Voltage profile of bus 32 under the solar irradiance of 9/8/2013 (SI_1).

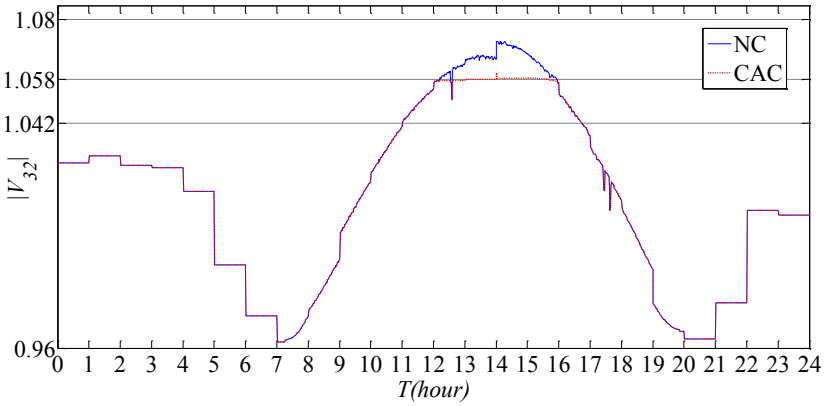

(b) Voltage profile of bus 32 under the solar irradiance of 9/10/2013 (SI_2).

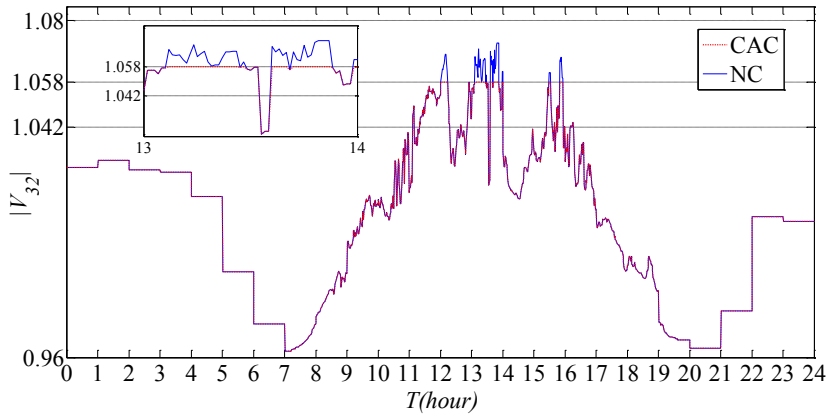

(c) Voltage profile of bus 32 under the solar irradiance of 9/19/2013 (SI_3).

Figure 10. Voltage profile of bus 32 under uniform solar irradiances.

3.4.1.2 *Diverse solar irradiance*

This case is used to simulate the scenario that different locations in the system may have different solar irradiances though the area covered by a distribution network is normally not large. In the simulation study, the three typical SI curves in Figure 3.5 are used for three different groups of PVs, i.e., SI_1 for the PVs at buses 1-10, SI_2 for the PVs at buses 11-20 and SI_3 for the PVs at buses 21-32. The voltage profiles of bus 32 with no control (NC) and the CAC method are shown in Figure 3.8. The voltage profile is also very good with the CAC in the sense that the voltage has been regulated as close to the upper bound as possible to generate more power from PVs without triggering the overvoltage protection. This result further demonstrates the effectiveness of the CAC method even when the PVs in the system experience diverse solar irradiances.

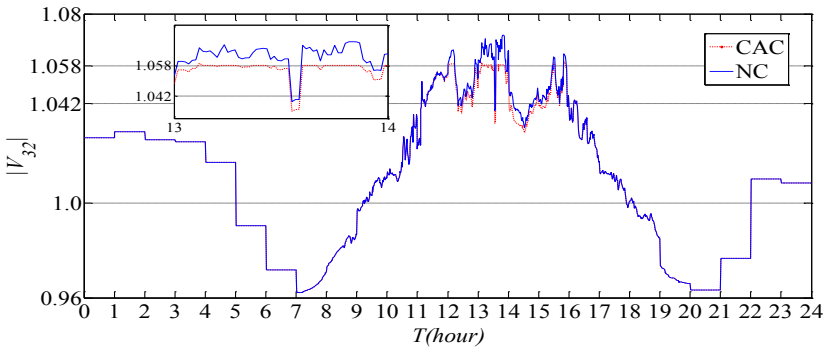

Figure 11. Voltage profile of bus 32 with diverse solar irradiances over the system.

3.4.1.3 *Comparative Analysis of V-Q control*

The proposed CAC method is compared with V-Q control methods under the scenario of diverse solar irradiances. It is assumed that the power factor of each PV generator can be altered in the range of ±95%. The V-Q control curve in [34] is used and shown in Figure 3.9 (a). In this figure, only V_3 and V_4 (set as 1.042 and 1.058 p.u., respectively) are used for overvoltage control. V_1 and V_2 in the figure are used for undervoltage control, which are not

discussed here. The voltage profile of the critical bus 32 is given in Figure 3.9 (b). It can be clearly seen that the V-Q control results in relatively large voltage fluctuations compared with the CAC method. Meanwhile, the voltage curve with the V-Q control method will frequently go over the upper limit of 1.058 p.u., indicating that the V-Q control cannot completely avoid overvoltage issues since the fixed V-Q control curve cannot always closely follow the changing system states.

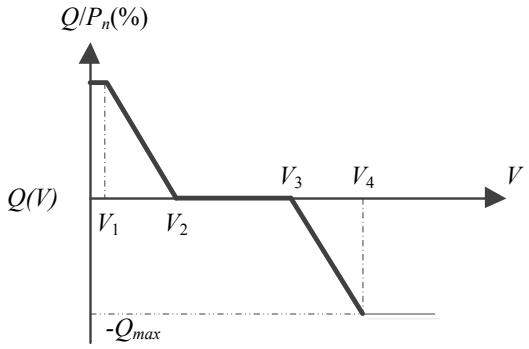

(a) V-Q control curve (V_3=1.042p.u., V_4=1.058p.u.) [2.34].

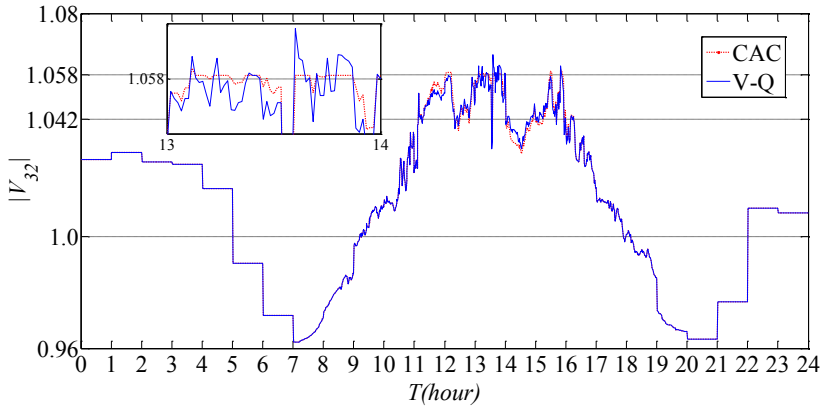

(b) Voltage profile of bus 32.

Figure 12. V-Q control with diverse solar irradiances over the system.

3.4.1.4 *Impact of Network Structure Change*

In order to explore the impact of network structure change on the proposed method, it is assumed that line 24/28 in Figure 3.4 is in service in the initial phase of simulation; and then it is disconnected from the system at 1:00 pm and stays off for the rest of 24-hour simulation period. The voltage profile of the critical bus and the real power output of the PV generator on the bus are shown in Figure 3.10 (a) and (b). Figure 3.10 (a) shows that the overvoltage can be effectively regulated below the upper limit of 1.058 p.u. Therefore, the proposed CAC method still works even after the network structure has changed. Meanwhile, according to Figure 3.10 (b), it is observed that the reference power (see (3)) of the PV at bus 32 changes from 0.1816 MW to 0.1781 MW after line 24/28 is disconnected. This indicates the adaptive nature of the CAC method and that the value of PV power caps will be updated in the process of changing system structure and state.

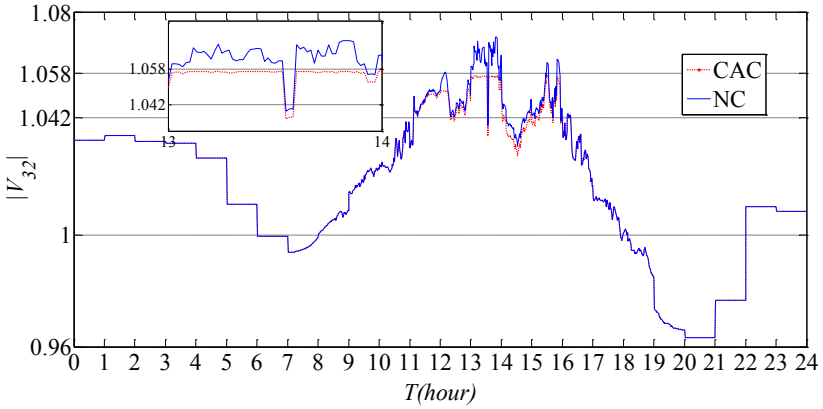

(a) Voltage profile

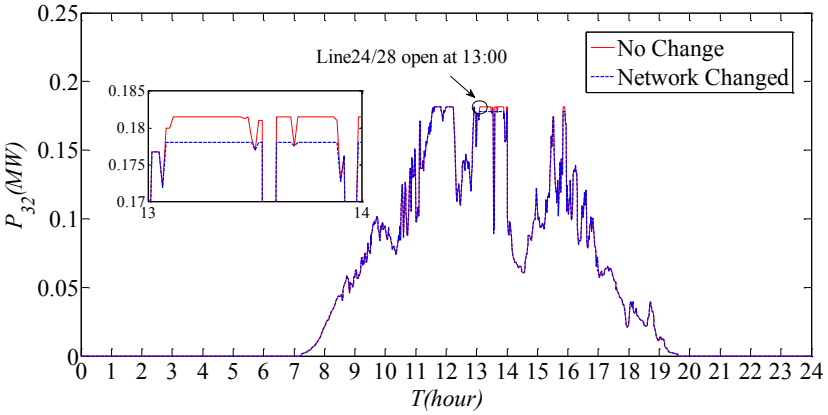

(b) PV output

Figure 13. Voltage profile and real power output under a network stucture change.

3.4.1.5 Consensus Control (COC)

When the solar irradiance is not uniform over the entire network and if there is no central controller to coordinate the PVs, the consensus control can help achieve the fair sharing of power curtailment. In this work, fairness means that the output power of each PV is curtailed by the same percentage based on the MPPT power that the PV can generate, as indicated in (2.11), (2.17) and (2.18). In this case, it is assumed that the communication network follows the same topology of the feeder lines, as show in Figure 3.4. The communication links are all assumed to be bidirectional. For example, the PV at bus 3 can communicate with bus 2 and bus 4 while the PV at bus 17 can only communicate with bus 16. The percentage power curtailments of all the PVs at a specific time point (1:00 pm) and the power loss profile during the whole simulation period are given in Figures 3.11 and 3.12, respectively. Figure 3.11 shows that the consensus control can help realize the fair distributing of the active power curtailments. Furthermore, in the 24-hour simulation period, the energy loss of the COC method is 2.4181 MWh, which is just slightly more than the total energy loss (2.4118 MWh) of the CAC method.

As an example, the voltage curve of bus 32 under the COC method is shown in Figure 3.13. The figure shows that the COC can effectively regulate the bus voltage below the pre-set upper limit while also achieving the fair sharing of power curtailments.

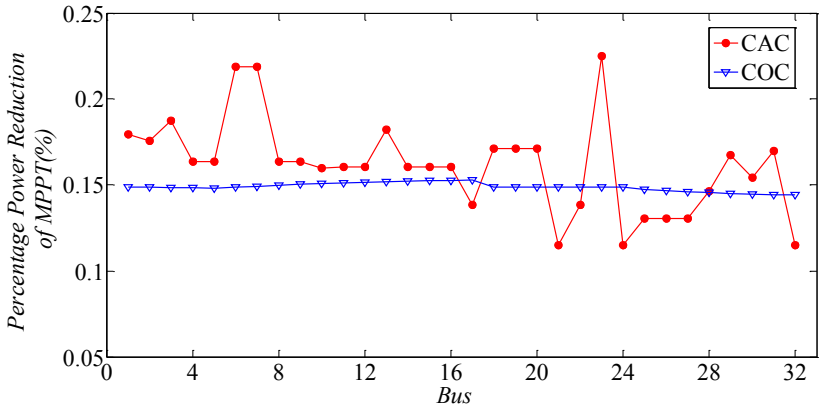

Figure 14. Percentage of power reduction.

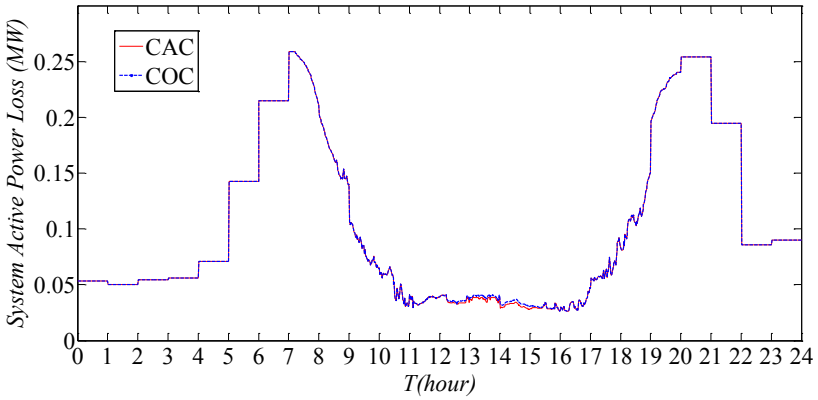

Figure 15. System active power loss.

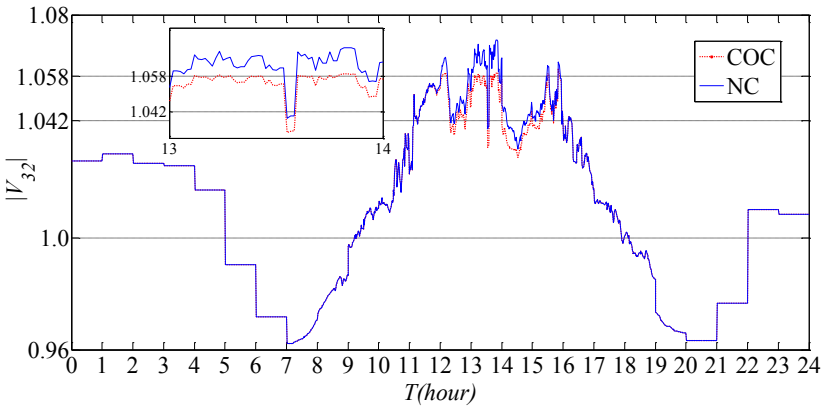

Figure 16. Voltage profile under the COC control.

3.4.2 Dynamic simulations

The effectiveness of the proposed power capping control and consensus control has been further verified through dynamic simulations. The simulations are carried out on the IEEE 13-bus test feeder [131] by using Simulink/SimPowerSystems [132]. As shown in Figure 3.14, some modifications are made to the original standard test system by adding two 1.5 MW PV generation systems at buses 675 and 680, respectively. The model and control of the PVs are adapted from [133]. The PV is connected to a DC/DC converter with MPPT control and then a DC/AC inverter with *dq*0 based PQ control [133]. The PV generation systems are operated in a unity power factor control mode, which means only real power control is considered. The output powers of the PVs follow the references provided by the CAC and/or the COC control.

There is a voltage regulator with LTC at bus 650 in the test system to regulate the bus voltage at 1.04 p.u. The LTC has 16 taps and a tap selection time of 8 s. In order to better observe the performance of the proposed methods, the LTC is first locked in the condition of no control. In other words, under this condition, the CAC or the COC method regulates the voltage profile by itself without the LTC. The impact of LTC will be investigated and discussed in the later portion of this sub-section.

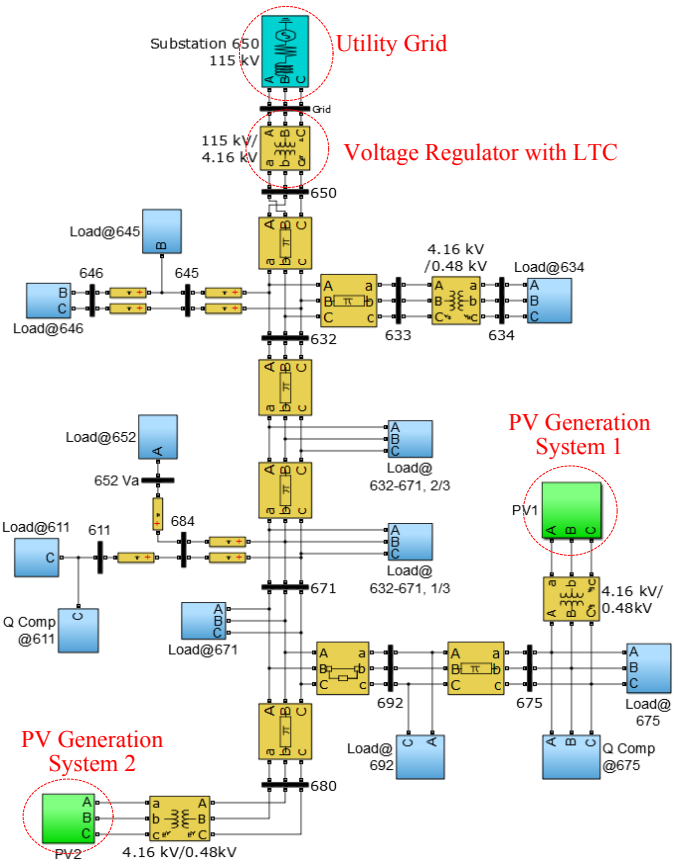

Figure 17. IEEE 13-bus test feeder system in Matlab/Simulink [134].

The changes of solar irradiances at buses 675 and 680 are shown in Figure 3.15. For the solar irradiance at bus 680, it starts to rise from 1% at t=1s and reaches 100% (100% means 1000 W/m^2 solar irradiance in the study) at t= 21s; then it stays at 100% for 5s and then takes 20s to decline back to 1%; 5s later it starts rising to 100% again. By using a very high ramp rate, from 1% to 100% in 20 s, the performance of the CAC and the COC control for voltage regulation is tested under a relatively extreme condition. In addition, the solar irradiance at bus 680 is assumed to be the same as the one at bus 675 but with a 5s delay.

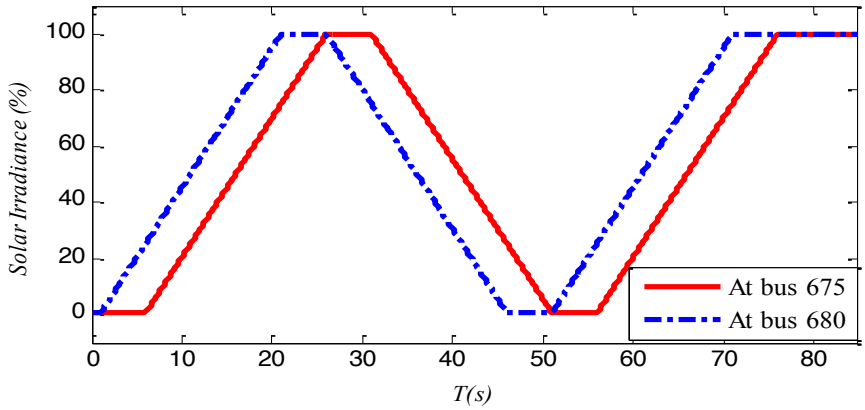

Figure 18. Solar irradiances in the dynamic simulations.

Since the studied system is three-phase unbalanced, the power curtailment via the CAC and/or the COC control is triggered whenever any of the three phases has reached the upper bound voltage. Consequently, the real power references are calculated according to the phase with the highest voltage by using (2.2) and (2.9). It is observed that the highest voltage occurs at phase A of bus 675. The voltage curves of V_{675A} under the conditions of no control, the CAC, and the COC control are shown in Figure 3.16. It shows that without any control the voltage goes beyond the upper bound, which can trigger the overvoltage protection to cut the PV system from the distribution grid. In addition, as shown in Figure 3.16, the highest voltage is regulated precisely just below 1.058 p.u. by the CAC control while the voltage under the COC control is slightly higher than the upper bound. The phenomenon that the bus voltage is slightly over the upper bound voltage under the COC control is because of the real power re-distribution between the two PVs. The real power re-distribution is shown in Figure 3.17. The COC control curtails the real power of PVs at 675 and 680 by the same percentage, as shown in Figure 3.17, which is the middle curve between the curtailment percentage curves of the PVs at 675 and 680 under the CAC control.

In addition, the proposed algorithms are compared with the LTC regulation and the result is also give in Figure 3.16. As shown in the figure, because of the delay in tap selecting, the LTC could not regulate the voltage within the security range fast enough under the scenario with rapidly changing solar irradiance. Large fluctuations of solar irradiance can also cause too many operations of the LTC, which could shorten the life of LTC and increase the cost of operation and maintenance.

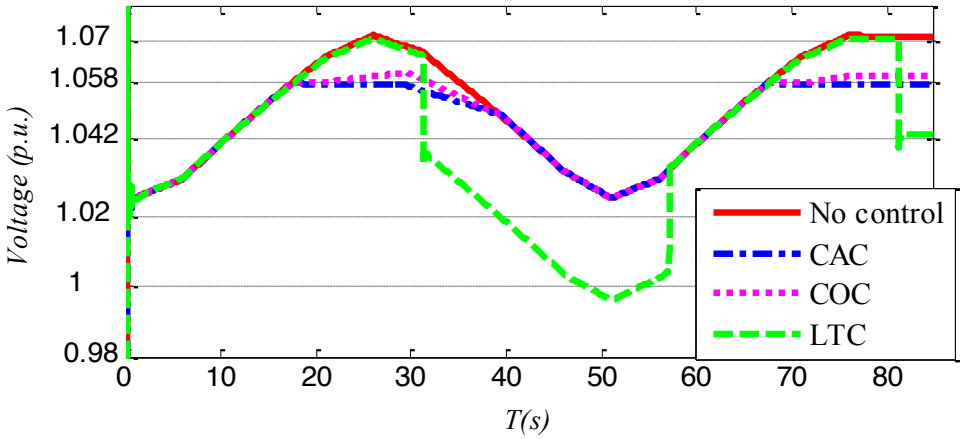

Figure 19. Profile of V_{675A} under three conditions: No control, CAC, COC, and LTC.

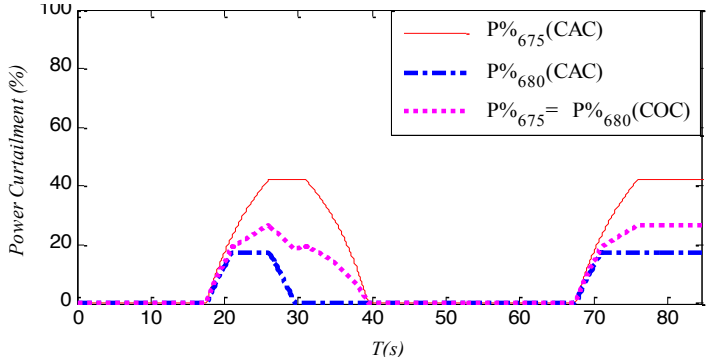

Figure 20. Percentage of power curtailments at 675 and 680 under the two control methods:(a) CAC control and (b) COC control.

To ensure the voltage security in the COC control, the action threshold voltage $V_{c,2}$ is reduced to 1.054 p.u. The simulation result of the voltage, V_{675A}, is shown in Figure 3.18. It can

be seen that the voltage is well regulated below 1.058 p.u. by tightening the action threshold voltage.

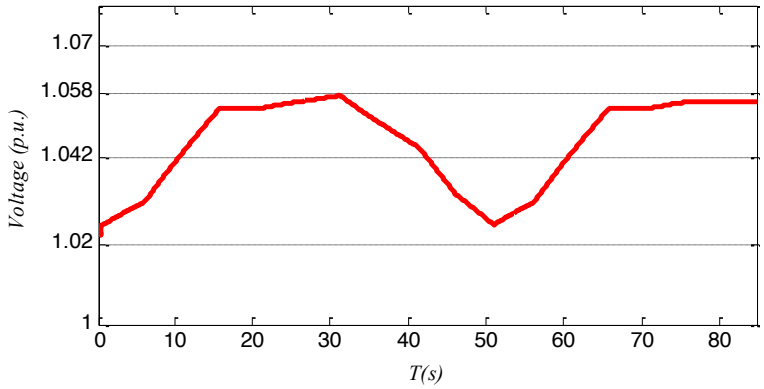

Figure 21. Variation of V_{675A} in the COC control with a lowered action threshold voltage.

From the dynamic simulation results, it can be seen that the CAC control is able to regulate the voltage under the upper bound. In addition, the results also verify that the COC control can help achieve the fair power curtailments even under dynamic situations.

3.5 Conclusion

For distribution networks with high penetration of PVs, it is important to not only regulate the voltages within an acceptable range, but also to fully utilize the PV generation capacity and to guarantee fair customer participation. An adaptive real power capping method was presented in this work to prevent overvoltages due to high penetration of PVs. The method uses local voltage and power measurements and does not require global information of a distribution network to calculate the output real power references/caps in real time for all the PVs in the system. The procedure was given and discussed to achieve the fairness in generation and power curtailment by either a centralized or distributed consensus control with limited communication capability. Simulation studies have been carried out on a 33-bus system for various scenarios including uniform and diverse solar irradiance distributions over the

network. Compared with the V-Q control method, the simulation results showed that the proposed method can effectively manage the voltage profile while assuring the fair share of power curtailments among the PVs even under network structure changes. The effectiveness of the method was further verified by the dynamic simulation studies on the IEEE 13-bus test feeder with unbalanced phases.

CHAPTER 4 DEVELOPMENT OF AUTONOMOUS SCHEDULES OF CONTROLLABLE LOADS FOR COST REDUCTION AND PV ACCOMMODATION IN RESIDENTIAL DISTRIBUTION NETWOK

4.1 Introduction

Load management, also called demand side management (DSM), has been considered as an important tool for managing future active distribution networks [135]. It is also a very useful measure for the economic, secure and environmentally friendly operation of bulk power systems [136], [137]. However, many of the load management strategies are focused on the interactions between and utility company and end users so that the end users can receive signals such as price, stability, and/or emission signals from certain central controllers to accomplish the load management process [103], [138]. Though significant advancements have been achieved in smart distribution network technologies, the appropriate platform and policy are not yet available for the majority of individual customers to receive those signals for a meaningful and guided load management [139]. Autonomous load management strategies with or without communicating the utility company have caught more attention recently [140], [141]. Actually, certain fixed time scheduling programs such as critical-peak pricing (CPP) and time-of-use pricing (ToUP) have been deployed for a while [140], [142]. For those programs, the utility company sets the prices for peak hours and off-peak hours while the end users choose to respond or not based on their own needs and preferences. Though those programs may not require the direct communication between end users and the utility company [140], there was a lack of certain flexibility and the characteristics of different loads were not considered. An advanced autonomous demand side management was proposed in [140] based game theory, but it requires bi-directional communications among all the users. An

autonomous load management scheme consisting of three layers, i.e., admission control, load balancing, and demand response management, was proposed in [141] for managing loads in smart buildings. However, the communication among local control entities is a necessary requirement to implement such scheme. An interesting smart phone based application that delivers environmental information associated with electricity usage at specific location and time has been developed and can be used for environmentally informed load management [141, 143]. Though this method does not require the communication between end users and the utility company directly, each user needs to have Internet access to retrieve data from a web based server [143].

The penetration level of photovoltaic (PV) generation has also been steadily growing in residential distribution networks around the world. Overvoltage is one of the most significant concerns for distribution networks with high penetration of PVs since it is not only a power quality issue but also a problem that can lower system reliability and the utilization level of PV generation [144, 145], [145]. It is desirable to utilize load management to assist the management of PVs.

The goal of this work is to develop typical schedules for controllable residential loads without receiving command signals from utility companies. For a given type of controllable load, six typical load management schedules will be developed for a given location, corresponding to six different combinations of seasons and week dates, i.e. three seasons of winter, summer and shoulder for weekdays and weekends. This methodology will help customers reduce their cost of electricity usage while assisting the management of possible PVs installed in the same distribution network.

The remainder of the chapter is organized as follows: The discussion on the proposed methodology and the problem formulation is given in Section 4.2. The algorithm implementation and the results are given in Section 4.3. The conclusion remarks and some discussions for the future work are given in Section 4.4.

4.2 Methodology and Problem Formulation

Three types of controllable loads (intelligent appliances), i.e., electric water heaters, refrigerators deicing loads, and dishwashers, are considered first in the work. These controllable loads have different characteristics and act as good examples to start with to develop autonomous, daily operation schedules. The methodology discussed later on in this section can be readily extended to other controllable loads such as plug-in electric vehicles. For a given location, based on statistical analysis of the locational marginal price (LMP) information and solar irradiance of that location, typical schedules will be developed for each type of load for the three different seasons during weekdays and weekends to achieve maximum likelihood of cost reduction while also reserving the load management resources to manage potential overvoltage issues due to high penetration of PVs. In general, it is an optimization problem with an objective to reduce cost and to maximize the PV utilization. The operation requirements and characteristics of each type of load can be converted into the constraints for the optimization problem.

4.2.1 Dishwasher P_1

The power dissipated by a dishwasher is represented by:

$$P_1(t_i) = t_i P_{dw}, \quad 1 \leq i \leq 24 \tag{4.1}$$

where P_{dw} is the dishwasher power, which is assumed to be a constant; t_i are binary values for 24 hours, i.e. $t_i = 0, or\ 1$. $t_i = 0$ means that the device should be turned OFF or be kept

staying at OFF position in that hour. $t_i = 1$ is for turning the device ON or keeping it at ON position.

$$\sum_{i=1}^{24} t_i = 2 \tag{4.2}$$

$$(2t_{24} - t_1 - t_{23}) < 2, or \ \leq 1$$

$$(2t_1 - t_2 - t_{24}) < 2 \tag{4.3}$$

$$(2t_i - t_{i+1} - t_i) < 2, \quad 2 \leq i \leq 23$$

$$\sum_{i=17}^{20} t_i = 0 \tag{4.4}$$

Eqs. (4.2) and (4.3) are used to represent the condition that the dishwasher needs to take two consecutive hours to finish the cleaning work. Eq. (4.4) indicates that the cleaning work has to be done before 17:00 o'clock in the day.

4.2.2 Refrigerator deicing P_2

The power consumed in 24 hours by the refrigerator deicing (RD) is given by:

$$P_2(t_i) = t_i P_{rd}, \ \ 1 \leq i \leq 24 \tag{4.5}$$

where P_{rd} is the refrigerator deicing demand power. The following conditions need to be met for the deicing power cycles in a day:

$$\sum_{i=1}^{24} t_i = 2 \tag{4.6}$$

$$\sum_{i=1}^{12} t_i = 1, \sum_{i=2}^{13} t_i = 1, \cdots, \sum_{i=13}^{24} t_i = 1. \tag{4.7}$$

Eqs. (4.6) and (4.7) represent the condition for having two deicing procedures in 24 hours and only one deicing process in 12 hours.

4.2.3 Electric water heater P_3

The power dissipated by an electric water heater (EWH) is represented by:

$$P_3(t_i) = t_i P_{ewh}, \quad 1 \leq i \leq 24 \tag{4.8}$$

Where P_{ewh} is the WEH power. The following conditions needed to be met for an electric water heater in a day:

$$\sum_{i=1}^{24} t_i = 4 \tag{4.9}$$

$$\sum_{i=1}^{9} t_i \leq 2, \sum_{i=2}^{10} t_i \leq 2, \cdots, \sum_{i=16}^{24} t_i \leq 2. \tag{4.10}$$

$$\sum_{i=1}^{5} t_i \leq 1, \sum_{i=2}^{6} t_i \leq 1, \cdots, \sum_{i=20}^{24} t_i \leq 1. \tag{4.11}$$

Eq. (4.9) represent the condition that there have to be four hours for the electric water heater to ON to keep the water temperature within the appropriate range for use. Eq. (4.10) indicates that the EWH cannot be heated more than twice in 9 hours while Eq. (4.11) says that the water heater can be not be heated more than 1 time in 5 hours.

4.2.4 Load management for assisting PV management

The stochastic analysis of solar irradiance is utilized to find the hour of the most possible solar irradiance peak in a day for the three seasons (i.e. winter, summer and shoulder). The

most possible solar irradiance peak hour is denoted as T_{PV}. There can be two ways of utilizing this PV peak hour information. One of them is to reduce the corresponding LMP values for the hour interval $[T_{PV} - 1, T_{PV} + 1]$ to give more incentives for the customer to use electricity during the PV peak hour(s), as indicated in (4.12). The actual value of incentive Δ can be set by the user.

$$LMP_i = \begin{cases} LMP_i - \Delta, if\ t_i \in [T_{PV} - 1, T_{PV} + 1] \\ LMP_i, \quad otherwise \end{cases} \tag{4.12}$$

The other way is to reserve certain load management resources for managing possible PV overvoltage issues by adding the following constraints:

$$\sum_{i=T_{PV}-3}^{T_{PV}-1} t_i = 0. \tag{4.13}$$

(The above constraint means that there is no load to be turned ON three hours before the PV peak hour so that the loads can be possibly turned ON during PV peak hour. The constraint the can be applied to some controllable loads or all of them.

The overall optimization problem can be formulated for the each season and week date combination as follows:

$$min\ C = \sum_{k=1}^{m} \left(\sum_{t_i=1}^{24} P_k(t_i)\, LMP_i \right) \tag{4.14}$$

Subject to the constraints in

$$(4.2) - (4.4), (4.6), (4.7), (4.9) - (4.11), \text{or } (4.13)$$

4.3 Algorithm Implementation and Scheduling Results

The above algorithm has been implemented using Matlab. For any location where the historical electricity price and solar irradiance data are available, the proposed can then be applied for that location. For areas covered by electricity markets, it is convenient to use LMP, which is archived and made available to public [146]. City of Lancing in the State of Michigan is chosen as the area of study. LMP data was collected from Midcontinent Independent System Operator (MISO) [146], and solar irradiation was taken from National Renewable Energy Laboratory (NREL) [147]. Statistical analysis was carried out for the LMP and solar irradiance data of the whole year of 2013 for the chosen location. The price distribution of each hour in a day was divided into six combinations according to the three seasons and two weeks' date options. Seasons were grouped as follows: December, January and February for winter, June, July, August and September for summer and March, April, May, October, and November for shoulder. The averages of 24 hours prices were calculated for each season. Moreover, solar irradiation data was treated into the same groups but this was calculated to show the solar irradiation peak. The six typical schedules can then developed for each of the three aforementioned appliances.

The average LMP curves over 24 hours for the three seasons are shown in Figures 4.1-4.3. It is clearly shown that different seasons have different sets of LMP curves. For the LMP curves of the winter season, it is clearly seen a bi-mode shape of curves. Moreover, two different curves o LMP were obtained for weekdays and weekends in all the seasons. LMP in the summer season hits $50 at 2pm and 4pm in weekdays while it was under $39 at 6pm in weekends in 2013, as shown in Figure 4.1.

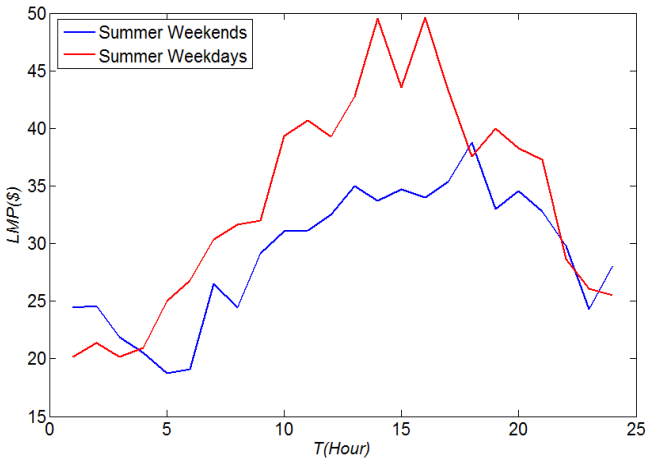

Figure 22. LMPs on the weekdays and weekends in the summer season.

As shown from Figure 4.2 of the winter season, the peak load happened at 7 pm, which was $41 in weekends while it was at 9 pm in weekdays.

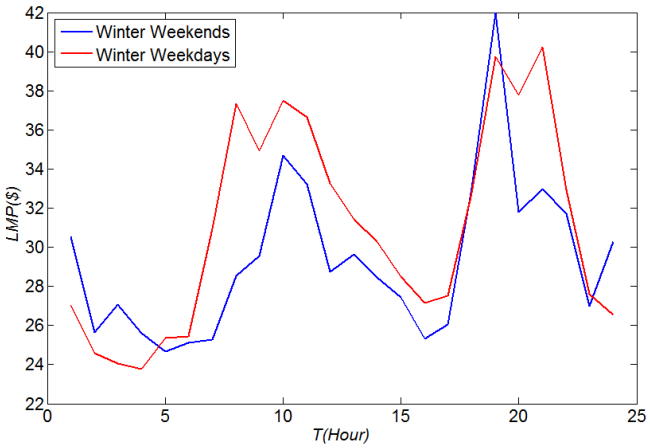

Figure 23. LMPs on the weekdays and weekends in the winter season.

In the shoulder season, the average price for weekdays reached $50 at 8pm but it was $40 in weekends, shown in Figure 4.3.

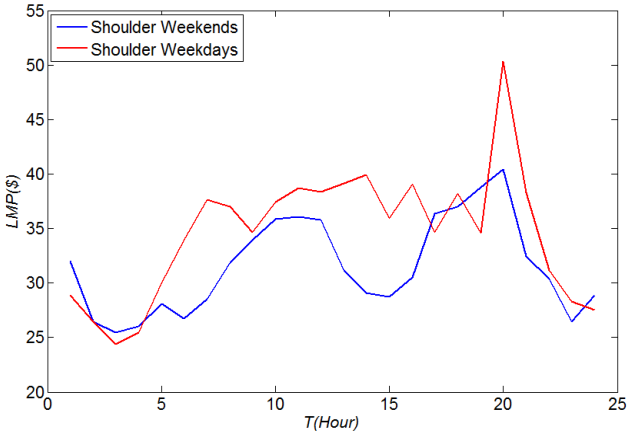

Figure 24. LMPs on the weekdays and weekends in the shoulder season.

4.3.1 Appliances Management

The autonomous schedules for dishwashers, refrigerator defrosts and electric water heaters have been developed according to the method given in Section 4.2. The scheduling results are given in Tables 4.1 – 4.8, where the PV management is not considered yet. The users can reduce their costs while without sacrificing their comfort. The users of the proposed schedules would save more than 50% of the energy consumption for these intelligent appliances. As the electric water heater works four hours a day, the optimization results for the shoulder season as example show that the best hours in weekdays are 12 am, 3 am, 9 am, and 7 pm while they are 2 am, 7 am, 3 pm and 11 pm, as shown in Table 4.1.

On weekdays in the summer season, the electricity price from the historical data was higher than the other seasons. The operation time selections for the EWH in weekdays are 1 am, 6 am, 6:00 pm and 12:00 am. On the other hand, the time slots preferred are scheduled to be 2 am, 7 am, 11 am and 12:00 am in weekends, as shown in Table 4.2.

Table 4.1 EWH hourly action profile for shoulder season

Time (h)	Weekdays	Weekends	Time (h)	Weekdays	Weekends
1	OFF	OFF	13	OFF	OFF
2	OFF	ON	14	OFF	OFF

3	ON	OFF	15	OFF	ON
4	OFF	OFF	16	OFF	OFF
5	OFF	OFF	17	OFF	OFF
6	OFF	OFF	18	OFF	OFF
7	OFF	ON	19	ON	OFF
8	OFF	OFF	20	OFF	OFF
9	ON	OFF	21	OFF	OFF
10	OFF	OFF	22	OFF	OFF
11	OFF	OFF	23	OFF	ON
12	OFF	OFF	24	ON	OFF

Table 4.2 EWH Hourly action Profile for the summer season

Time (h)	Weekdays	Weekends	Time (h)	Weekdays	Weekends
1	ON	OFF	13	OFF	OFF
2	OFF	ON	14	OFF	OFF
3	OFF	OFF	15	OFF	OFF
4	OFF	OFF	16	OFF	OFF
5	OFF	OFF	17	OFF	OFF
6	ON	OFF	18	ON	OFF
7	OFF	ON	19	OFF	OFF
8	OFF	OFF	20	OFF	OFF
9	OFF	OFF	21	OFF	OFF
10	OFF	OFF	22	OFF	OFF
11	OFF	ON	23	OFF	ON
12	OFF	OFF	24	ON	OFF

On the winter weekdays, EWH worked twice in the early morning because customers would take showers and the water consumption was high. The price schedule was optimized to operate at 1 am, 6 am, 4 pm, and 12 am while the operation of the water heater on weekends was set to be at 2 am, 7 am, 3 pm and 11 pm, as shown in Table 4.3.

Table 4.3 EWH Hourly action Profile for the winter season

Time (h)	Weekdays	Weekends	Time (h)	Weekdays	Weekends
1	ON	OFF	13	OFF	OFF
2	OFF	ON	14	OFF	OFF
3	OFF	OFF	15	OFF	ON
4	OFF	OFF	16	ON	OFF
5	OFF	OFF	17	OFF	OFF
6	ON	OFF	18	OFF	OFF
7	OFF	ON	19	OFF	OFF
8	OFF	OFF	20	OFF	OFF
9	OFF	OFF	21	OFF	OFF
10	OFF	OFF	22	OFF	OFF
11	OFF	OFF	23	OFF	ON
12	OFF	OFF	24	ON	OFF

The two consecutive hours of dishwasher operation were at 3 am and 4 am on weekends and weekdays, which were optimized to meet the goal for the shoulder season as shown in Table 4.4.

The operation of dishwasher in the summer and winter seasons had the same time of duty for weekdays and weekends. The time of operation on weekdays was assigned to 3am, and 4am; in contrast, 5am and 6am was the time operation on weekends for the both seasons. Moreover, the weekdays of the three seasons had the same schedule of operation as shown in Table 4.5.

Table 4.4 Dishwasher Hourly action Profile for the shoulder season

Time (h)	Weekdays	Weekends	Time (h)	Weekdays	Weekends
1	OFF	OFF	13	OFF	OFF
2	OFF	OFF	14	OFF	OFF
3	ON	ON	15	OFF	OFF
4	ON	ON	16	OFF	OFF

5	OFF	OFF	17	OFF	OFF
6	OFF	OFF	18	OFF	OFF
7	OFF	OFF	19	OFF	OFF
8	OFF	OFF	20	OFF	OFF
9	OFF	OFF	21	OFF	OFF
10	OFF	OFF	22	OFF	OFF
11	OFF	OFF	23	OFF	OFF
12	OFF	OFF	24	OFF	OFF

Table 4.5 Dishwasher Hourly action Profile for the summer and winter season

Time (h)	Weekdays	Weekends	Time (h)	Weekdays	Weekends
1	OFF	OFF	13	OFF	OFF
2	OFF	OFF	14	OFF	OFF
3	ON	OFF	15	OFF	OFF
4	ON	OFF	16	OFF	OFF
5	OFF	ON	17	OFF	OFF
6	OFF	ON	18	OFF	OFF
7	OFF	OFF	19	OFF	OFF
8	OFF	OFF	20	OFF	OFF
9	OFF	OFF	21	OFF	OFF
10	OFF	OFF	22	OFF	OFF
11	OFF	OFF	23	OFF	OFF
12	OFF	OFF	24	OFF	OFF

The time slots selected in which the cost was low for the refrigerator deicing to be on was 6 am and 2 pm on the shoulder season weekends whereas it was 9 am and 7 pm on weekdays, as shown in Table4.6.

Table 4.6 RD Hourly action Profile for shoulder season

Time (h)	Weekdays	Weekends	Time (h)	Week-days	Week-ends
1	OFF	OFF	13	OFF	OFF

2	OFF	OFF	14	OFF	OFF
3	ON	ON	15	OFF	OFF
4	OFF	OFF	16	OFF	OFF
5	OFF	ON	17	OFF	OFF
6	OFF	ON	18	OFF	OFF
7	OFF	OFF	19	OFF	OFF
8	OFF	OFF	20	OFF	OFF
9	OFF	OFF	21	OFF	OFF
10	OFF	OFF	22	OFF	OFF
11	OFF	OFF	23	OFF	ON
12	OFF	OFF	24	ON	OFF

Table 4.7 RD Hourly action Profile for summer season

Time (h)	Weekdays	Weekends	Time (h)	Weekdays	Weekends
1	ON	OFF	13	OFF	OFF
2	OFF	OFF	14	OFF	OFF
3	OFF	OFF	15	OFF	OFF
4	OFF	OFF	16	OFF	OFF
5	OFF	ON	17	OFF	OFF
6	OFF	OFF	18	OFF	OFF
7	OFF	OFF	19	OFF	OFF
8	OFF	OFF	20	OFF	OFF
9	OFF	OFF	21	OFF	OFF
10	OFF	OFF	22	OFF	OFF
11	OFF	OFF	23	OFF	ON
12	OFF	OFF	24	ON	OFF

On the summer weekends, the refrigerator deicing had two intervals of operation in 24 hours, and the time slot for its operation was 5 am and 11 pm while it operated at 1am and 12 am on weekdays in order to decrease the bill according to the historical data of LMP, shown in Table 4.7.

In the winter season, RD was scheduled to work at 3 am and 11 pm on weekdays but it operated at 1 am and 12 am after midnights on weekends, shown in Table 4.8.

Table 4.8 RD Hourly action Profile for winter season

Time (h)	Weekdays	Weekends	Time (h)	Weekdays	Weekends
1	OFF	ON	13	OFF	OFF
2	OFF	OFF	14	OFF	OFF
3	ON	ON	15	OFF	OFF
4	OFF	OFF	16	OFF	OFF
5	OFF	ON	17	OFF	OFF
6	OFF	ON	18	OFF	OFF
7	OFF	OFF	19	OFF	OFF
8	OFF	OFF	20	OFF	OFF
9	OFF	OFF	21	OFF	OFF
10	OFF	OFF	22	OFF	OFF
11	OFF	OFF	23	ON	OFF
12	OFF	OFF	24	OFF	ON

4.3.2 Load management for assisting the accommodation of high penetration of PVs

The PV historical data in Figure 4.4 shows that the three seasons have peak at the same hour, i.e. 1 pm. The maximum solar irradiations for the winter, shoulder, and summer seasons are 600 W/m^2, 950 W/m^2, and 1200 W/m^2, respectively. The highest reverse power might happen in the summer season compared with the other seasons, which may fall between 12 pm to 2 pm, as shown in Figure 4.4. The duration of solar irradiations in the summer and the shoulder starts early of each day at 6 am and diminishes at 8 pm; in contrast, the period of solar irradiations in winter are nine hours. The three intelligent appliances would be operated in this period of time according to consumers' choice and the actual installed PV capacity. But the probability of operation would be recommended between the three hours of peak.

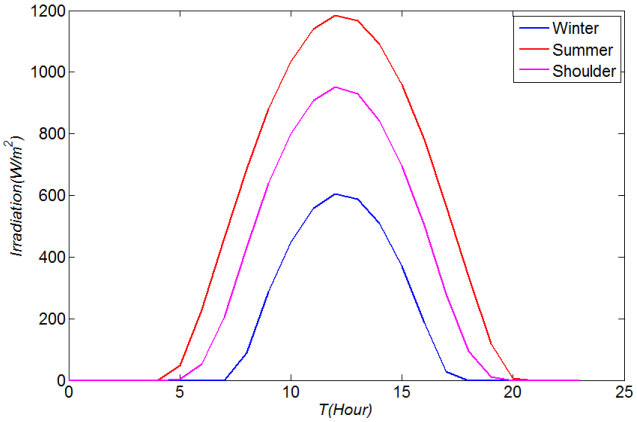

Figure 25. Solar irradiation for the three seasons.

As the high penetration of PV would happen from 12pm to 2pm, and the consumers have a big value of power of PV generation, they can turn on their appliances to utilize PV's power, particularly when the regular loading level is low, as shown in Figure 4.5. A new set of scheduling results can be obtained similarly by incorporating the PV management in either of the two ways discussed in Section 4.2.4.

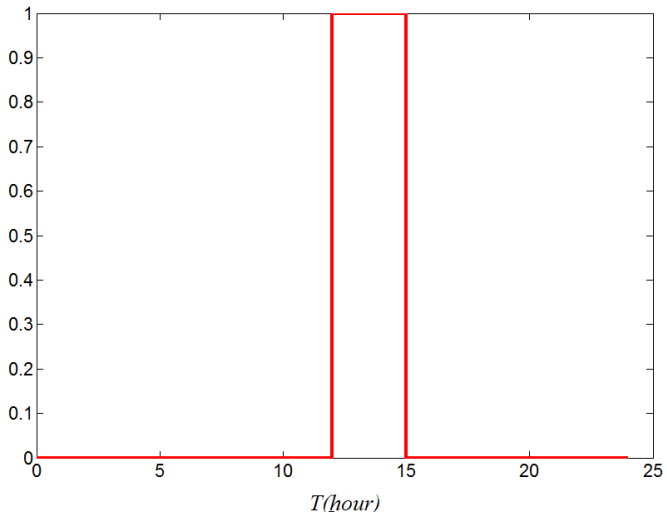

Figure 26. Appliances operation at maximum PV generation.

4.4 Conclusion

This chapter proposed a method to develop autonomous load management schedules for typical intelligent appliances without communicating with the utility company. Based on the

statistical analysis of the electricity cost and solar irradiance information for a specific location, the schedules have been developed for three types of loads and for the three different seasons during weekdays and weekends to achieve maximum likelihood of cost reduction while also reserving the load management resources to manage potential overvoltage issues due to high penetration of PVs. The scheduling results have been given and discussed for an example location chosen at Michigan with the data for year of 2013.

An interesting phenomenon that can be noted from Table 4.1 and 4.4 is that, for example, at 3:00AM, it is one of the optimal time slots scheduled for both the EWH and dishwasher. Though different areas may have different electricity price profiles that can result in different schedules, it is still possible that certain number of controllable loads may be activated based on the same or similar schedules and thus generate new peaks. To solve this problem, the communication among users will become necessary for a better coordination. Nevertheless, the developed autonomous schedules in this work can act a good alternative measure to start with.

CHAPTER 5 OVERVOLTAGE RISK ANALYSIS IN DISTRIBUTION NETWORKS WITH HIGH PENETRATION OF PVS

5.1 Introduction

Overvoltage is one of the most significant concerns among these emerging challenges. If not well designed, overvoltage can cause PV systems to be tripped off, affecting both the power delivery reliability and the PV owners' revenue. A number of interesting studies were carried out to discuss the voltage control capability of PVs [148], such as the power droop control (voltage versus power) methods [110], [44] and the sensitivity analysis methods [149], [150]. Meanwhile, a Thevenin equivalent-based method was presented in [151] and a consensus control method was proposed in [152] to manage overvoltage problems. The focus of all of these methods is on the real time operation after the PVs have been installed in a distribution network. However, when solar power has become paramount, there is a need to consider the overvoltage risk due to high penetration of PV from the beginning of planning phase.

Optimal sizing and siting of DG sources including PV has been discussed in many papers to minimize DG's investment, reduce operating costs, reduce power losses, improve voltage profiles, and to increase system reliability [15],[153]- [154]. For instance, a genetic algorithm (GA)-based approach for minimizing power losses in a network was proposed in [155]. A new integrated model for DG planning with multiple objectives of minimizing investment costs, operating costs and payment compensation for losses was proposed in [155]. In [156] power loss reduction and voltage profile improvement were considered together in the optimal model by using Harmony Search (HS) algorithm. System reliability was taken into account in [157] along with the goal to minimize network losses. Unlike the deterministic methods above, this

work aims at the probabilistic risk analysis of various distributed PV capacities in a distribution network under the consideration of intermittent solar irradiance.

From the point of planning, the performance of a distribution system depends on not only the electric characteristic of the distribution network, but also the stochastic characteristic of solar irradiance. In most cases, there is no single probability distribution that can match the characteristic of solar irradiance for every month in a whole year. It is necessary to find the probability density functions that can best describe the sunshine hours and irradiance for different months. Some probability density functions have been reported in literature to characterize solar irradiance distribution, such as normal function [158], lognormal function [159], gamma function[160], Weibull function [161], Exponential and Beta function [162] and Rayleigh function [163]. In this paper, the Kolmogorov–Smirnov test (K–S test) [164] is used to obtain the best distribution among a set of commonly used distributions for the solar irradiance data collected at a site in the USA.

This chapter is organized as follows: An iterative method is first proposed in Section 5.2 to calculate the maximum PV power injection in distribution networks under certain load profile. The method is based on the sensitivity analysis between active power injection and voltage magnitude and an iterative calculation process is introduced to increase the accuracy of algorithm. The probability distribution of solar irradiance is discussed in Section 5.3. This section also explains how to calculate the different risks regarding various PV sizes. An illustration example is given in Section 5.4 to verify the effectiveness of the proposed model and method, followed by the conclusion in Section 5.5.

5.2 Maximum PV Power Injection

5.2.1 Sensitivity Analysis

In this work, the first-order sensitivity analysis method in [149] is used to quantify the impact of the change of active power on the variation of voltage magnitude in a distribution network. The sensitivity matrix, also called Jacobian Matrix, can be obtained directly from Newton–Raphson load flow calculation [165].

$$\begin{bmatrix}\Delta P\\ \Delta Q\end{bmatrix} = \begin{bmatrix}J_{P\delta} & J_{PV}\\ J_{Q\delta} & J_{PV}\end{bmatrix}\begin{bmatrix}\Delta\delta\\ \Delta V\end{bmatrix} \tag{5.1}$$

As given in (5.1), the Jacobian Matrix is composed of four partial derivative submatrices reflecting the sensitivity of the active and reactive power injections versus the bus voltage magnitudes and angles. Only the overvoltage issue due to active power changes is discussed in this work. It is well known that the solar power ΔP is an important reason leading to overvoltage in distribution networks due to the high R/X rate of radial feeders. Therefore, it is reasonable to focus on active power injection capability for PVs, especially at the planning stage. Reactive power compensation methods for voltage support, such as capacitor placement and PV reactive power control capability are, therefore, not discussed here.

By assuming $\Delta Q = 0$ in (5.1), we have

$$0 = J_{Q\delta}\Delta\delta + J_{PV}\Delta V \tag{5.2}$$

$$\Delta\delta = -{J_{Q\delta}}^{-1}J_{PV}\Delta V \tag{5.3}$$

Substituting (5.3) into (5.1) to replace $\Delta\delta$ yields

$$\Delta P = (J_{PV} - J_{P\delta} J_{Q\delta}{}^{-1} J_{PV}) \Delta V \quad (5.4)$$

and

$$\Delta V = (J_{PV} - J_{P\delta} J_{Q\delta}{}^{-1} J_{PV})^{-1} \Delta P = S_{VP} \cdot \Delta P \quad (5.5)$$

where S_{VP} is the V-P sensitivity index which is used to quantify the impact of marginal changes of active power on the voltage magnitude variations.

5.2.2 Maximum Power Injection

In order to maximize the active power injection from PVs, the following incremental power optimal model is used,

$$max \sum_{i=0}^{N-1} \Delta P_i \quad (5.6)$$

s.t.

$$V_{lower,i} \leq V_i + S_{VP,i} \cdot \Delta P_i \leq V_{upper,i} \quad (5.7)$$

$$P_{lower,i} \leq P_{i+1} = P_i + \Delta P_i \leq P_{upper,i} \quad (5.8)$$

Where N is the total node number; P_i and V_i are the active power and voltage magnitude at bus i, which is obtained by solving power flow in simulation. The sensitivity index $S_{VP,i}$ can be also obtained in Newton–Raphson load flow calculation. The objective of the optimal model is to maximize power outputs from PVs, i.e., Eq. (5.6) while keeping the bus voltage and PV power output within the preset constraints, i.e., Eqs. (5.7) and (5.8).

In the above optimal model, a linear approximation method is used to evaluate the sensitivity between active power and voltage magnitude. In order to increase accuracy, an iterative procedure is implemented to calculate the maximum active power injection.

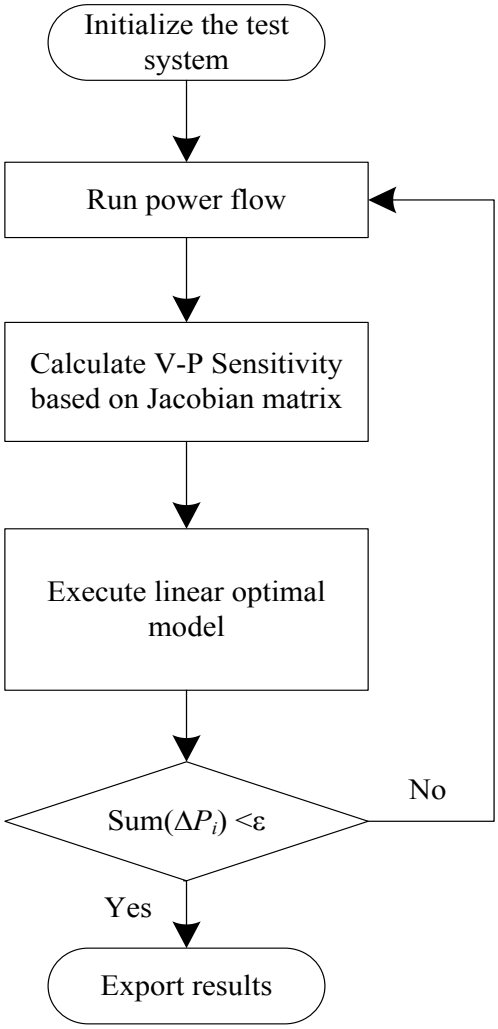

Figure 27. Iterative procedure to calculate the maximum active power injection.

In Figure 5.1, the whole system state including the V-P sensitivity index (S_{VP}) keeps updating in each iteration. The iterative procedure will continue until no more power injection can be added to the system. It means sum(ΔP_i)< ε, where ε is a small number. The simulation results in Section 5.4 will show the proposed model and method is accurate enough to find the maximum active power injection.

5.3 Probability Distribution of Solar Irradiance

PV placement in a distribution network is not only affected by the allowable active power injection of the distribution system, but also influenced by the stochastic characteristic of solar irradiance in the corresponding geographic area. For example, assuming that the typical solar irradiance in an area is 200W/m^2 and the allowable power injection from PVs in a distribution network in that area is 500kW, a PV system with a nominal capacity of 2500kW may be needed because the nameplate value is normally measured under the standard solar irradiance of 1000W/m^2. If the solar irradiance is often higher than 200W/m^2, we may need to reduce the PV capacity to avoid frequent overvoltage issues. On the other hand, if the solar irradiance is often lower than 200W/m^2, then a PV system with a larger nominal capacity can be installed without increasing the overvoltage risk.

5.3.1 Probability Distribution of Solar Irradiance

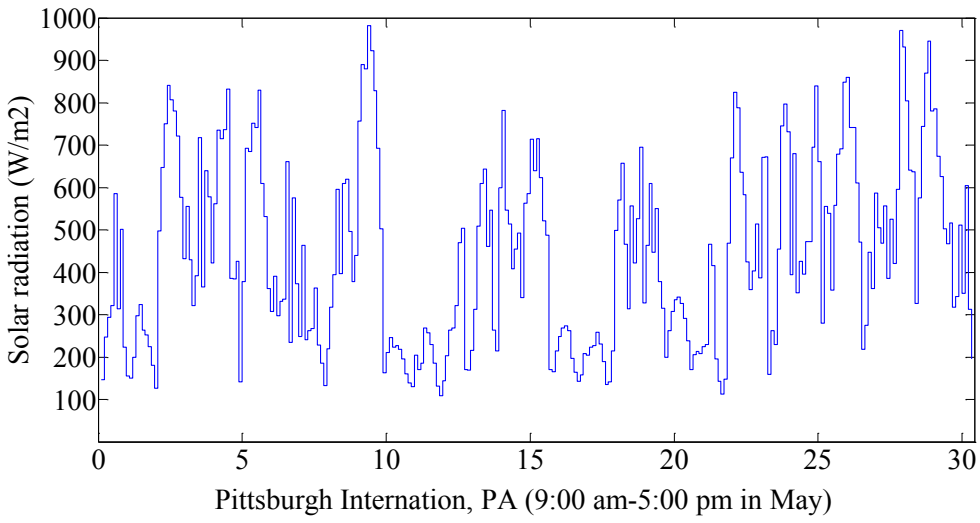

(a) May, 2010

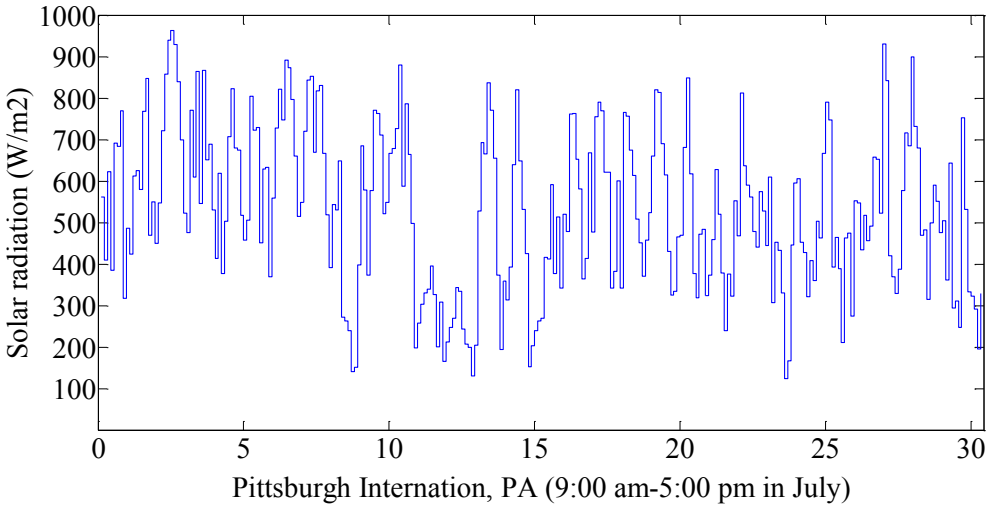

(b)July, 2010

Figure 28 Solar irradiance at Pittsburgh International Airport [29].

The solar irradiance data collected at Pittsburgh International Airport, in May and July 2010, are used as two examples to investigate characteristics of solar irradiance distribution. Shown in Figure 4.2, the data is obtained from the National Solar Radiation Data Base (NSRDB) [166] with an interval of 1 hour (i.e. 24 points each day). It is noted that only the data from 9:00 am and 5:00 pm are plotted in this figure and used in the following statistical test since the other hours have either no or low solar irradiance. It can be observed that the sunshine hours and solar irradiance values in May and July are different. Therefore there is a need to find the probability density function that best describes the solar irradiance probabilistic characteristic in each month in one year. The Kolmogorov–Smirnov test (K–S test) is used to obtain the best distribution among a set of commonly used distribution functions for each month in the year.

5.3.2 Kolmogorov–Smirnov test

The Kolmogorov–Smirnov test (K–S test) is a method used to identify whether a sample comes from a population with a hypothesized continuous distribution. The K–S test measures

the distance between the empirical cumulative distribution function (ECDF) of samples and the cumulative distribution function of the hypothesized theoretical distribution [167]. For an ordered solar irradiance sample sequence x_1, x_2 … x_n (from the smallest to the largest) following some distribution with a cumulative distribution function $F(x)$, the ECDF is defined by [30]:

$$F_n(x) = \frac{1}{n}\sum_{i=1}^{n} I(x_i) \tag{5.9}$$

$$I(x_i) = \begin{cases} 1 & x_i \le x \\ 0 & x_i > x \end{cases} \tag{5.10}$$

The K–S statistical value (D_n) for a given test cumulative distribution $F(x)$ is calculated by [30]

$$D_n = \sup_x |F_n(x) - F(x)| \tag{5.11}$$

A tested distribution is rejected if the test statistical value (D_n) is greater than a predefined critical value (D_{cr}). Otherwise, if D_n is smaller than the critical value, the tested distribution is accepted. Here, the p-value is adopted to answer what the probability is so that the two cumulative frequency distributions would be as close as observed, i.e., $P(D_n<D_{cr})$. If the p-value is small, it is concluded that the two groups are with different distributions. The details of the p-value method can be found in [168]. The p-value shows how well a tested distribution fits the observed dataset as an entire shape.

For the solar data collected at Pittsburgh International Airport, a total of eight hypothetic probability distributions have been tested by using the K-S method, i.e., the Normal function [169], the Lognormal function [157], the Gamma function [158], Weibull function [159], Exponential function and Beta function [160], Rayleigh function [161], and Rician function. The test results are listed in the Table 5.1 and Table 5.2 below.

Table 5.1 p-values in K-S test

p-values	Normal	Lognormal	Exponential	Weibull
Mon1	0.0001	0.0005	0.0204	0.5572
Mon2	0.0000	0.0003	0.0001	0.0123
Mon3	0.0003	0.0120	0.0000	0.3321
Mon4	0.0019	0.0429	0.0001	0.4573
Mon5	**0.0117**	**0.0052**	**0.0010**	**0.1822**
Mon6	0.0094	0.0009	0.0000	0.1628
Mon7	**0.5997**	**0.0000**	**0.0000**	**0.2964**
Mon8	0.1801	0.0001	0.0000	0.0420
Mon9	0.2087	0.0001	0.0000	0.0328
Mon10	0.0002	0.0017	0.0006	0.1972
Mon11	0.0004	0.0015	0.0003	0.4265
Mon12	0.0000	0.0001	0.0026	0.1103

Table 5.2 p-values in K-S test

p-values	Gamma	Beta	Rayleigh	Rician
Mon1	0.3226	0.4916	0.0000	0.0000

Mon2	0.0355	0.0043	0.0000	0.0000
Mon3	0.3793	0.2409	0.0000	0.0000
Mon4	0.5676	0.3118	0.0000	0.0000
Mon5	0.0437	0.5948	0.0000	0.0000
Mon6	0.0227	0.3898	0.0001	0.0001
Mon7	0.0143	0.5702	0.2323	0.5140
Mon8	0.0121	0.5036	0.0289	0.0244
Mon9	0.0229	0.1861	0.0486	0.0668
Mon10	0.0496	0.3280	0.0000	0.0000
Mon11	0.4024	0.6368	0.0000	0.0000
Mon12	0.1039	0.0797	0.0000	0.0000

It can be clearly seen that the distribution of solar irradiation at Pittsburgh International Airport varies monthly. For example, the solar irradiance in May follows the Beta distribution with parameters (α=1.9965, β=2.4623), while in July a Normal probability distribution (μ=0.5281, σ=0.1929) is proper to describe the variation of solar irradiance. The fitting curves of probability distribution for May and July are shown in Figure 5.3.

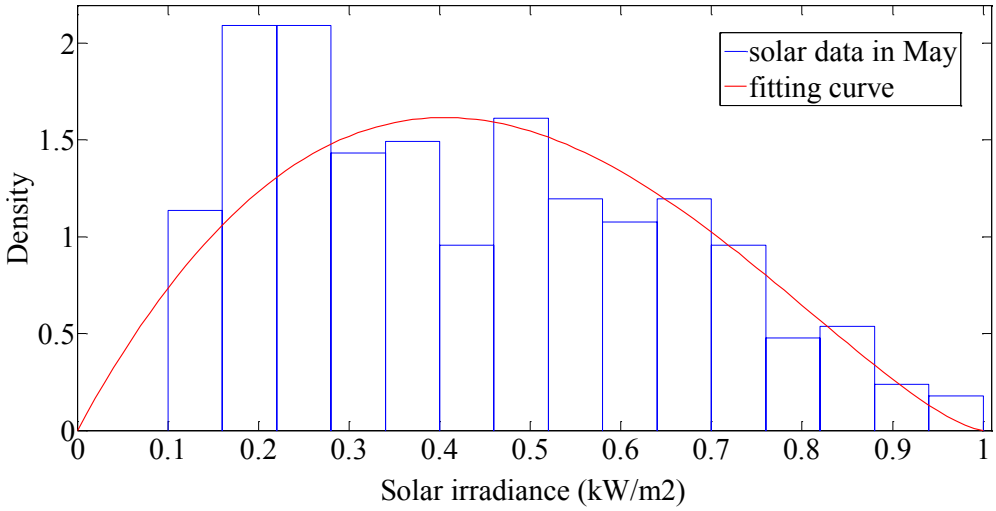

(a) Beta Distribution in May ($\alpha = 1.9965, \beta = 2.4623$)

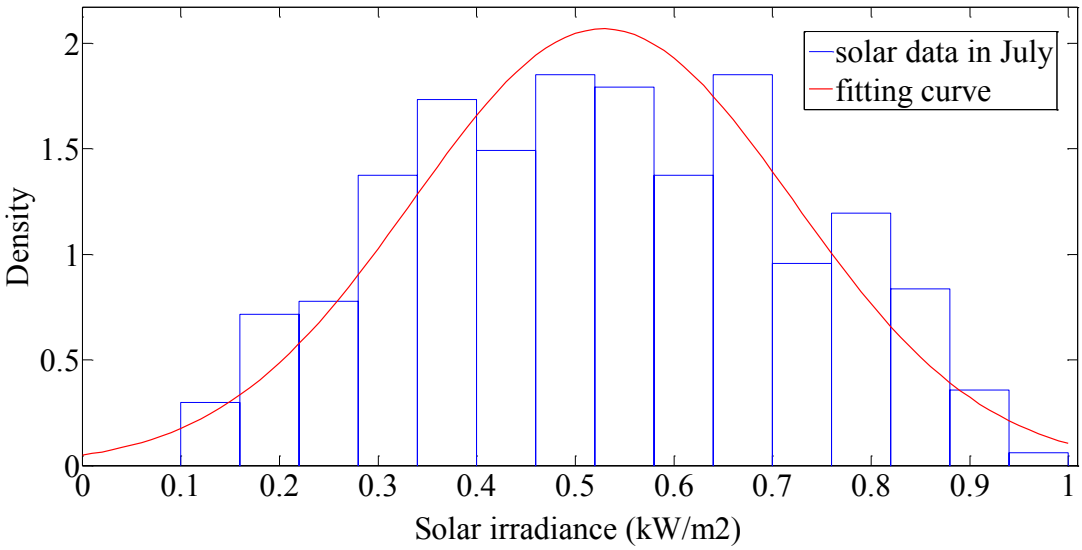

(b) Normal Distribution in July, 2010 ($\mu = 0.5281, \sigma = 0.1929$)

Figure 29. Fitting curves of the probability distributions of the solar irradiance at Pittsburgh International Airport.

5.3.3 Risk associated with PV size

Taking the system that allows 500kW power injection as an example, if a total of 2500kW PV capacity (i.e. the nameplate capacity under the condition of 1kW/m^2 solar irradiance) has

been installed in the system, the critical solar irradiance without trigging overvoltage would be 0.2kW/m^2. The overvoltage risk regarding the 2500kW PV capacity is, therefore, calculated as

$$P_{\text{risk}}(2500kW) = P(x > 0.2kW/m^2) \qquad (5.12)$$

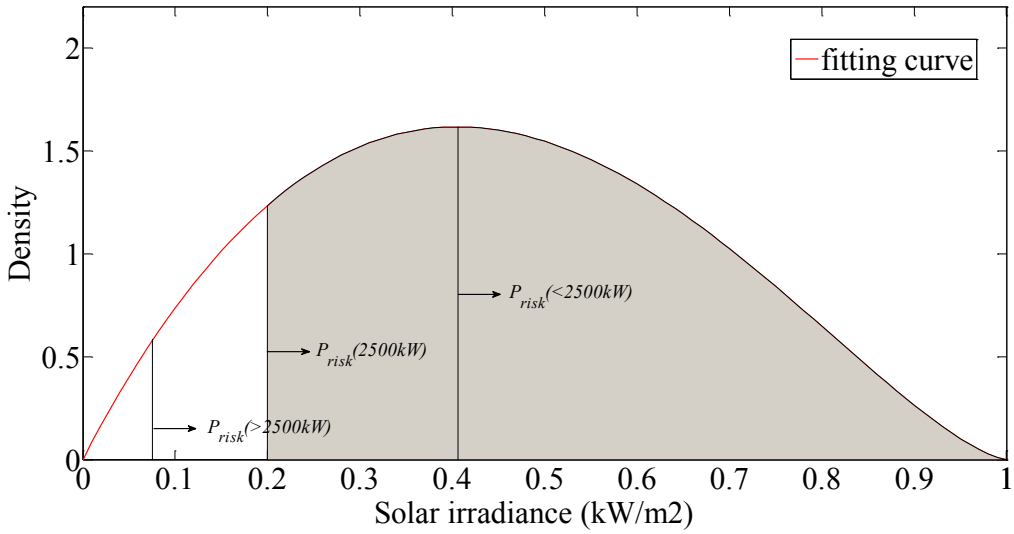

Figure 30 Probability of overvoltage risk.

Figure 5.4 shows a graphic representation of the overvoltage risk calculation. Obviously, installing more PVs lowers the critical value of allowable solar radiation that leads to higher overvoltage risk in the system. That means system operators have high chance to meet overvoltage issues during the active solar hours from 9:00 am to 5:00 pm.

5.4 Case Studies

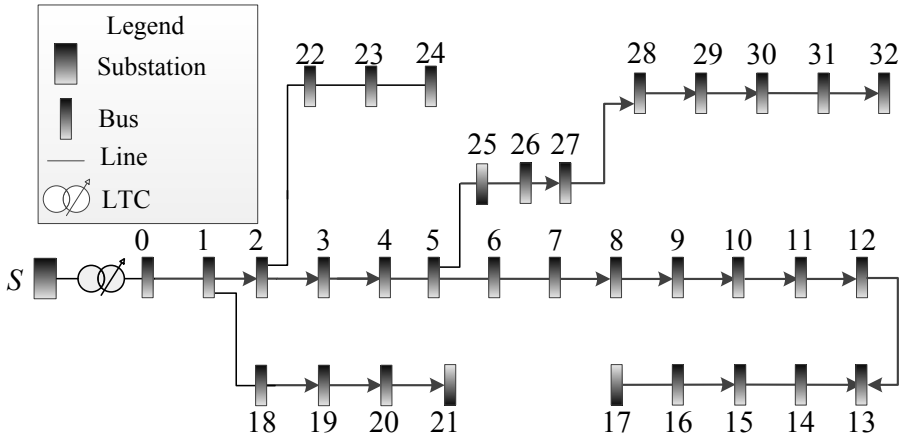

Figure 31 A 33-bus test system [32].

The proposed PV placement method and the corresponding overvoltage risk assessment are verified on a 33-bus system, shown in Figure 5.5 [168]. The system has a base load of 4.2 MW real power and 3 MVar reactive power. All the buses except bus 0 are potential locations to install PV. In order to avoid the PV capacity being only placed at the buses close to the substation (bus 0), the maximum power injection at each bus is limited to 500kW. The simulation results are given and discussed in the following of this section.

5.4.1 PV Placement under Various Load Levels

First, the incremental method in Figure 5.1 is used to decide the maximum safe DG injection power that will not lead to overvoltage problem. The load levels from 0.6 to 1.6 times of the base level are investigated. The corresponding maximum power injection and voltage magnitude at each bus are shown in Tables 5.2 and 5.3. The information is used in the next step of risk assessment to determine the proper PV capacity sizes.

As shown in Tables 5.2 and 5.3, the PVs are first placed on the buses with lower V-P sensitivity associated with the critical buses having overvoltage problems, such as buses 32 and 17. When the load level increases, more active power can be injected into the system. It is

noted from Table III that no bus voltage is higher than the predefined 1.05 p.u. critical value, indicating the effectiveness and accuracy of the proposed incremental iteration method.

5.4.2 Risk analysis for various PV sizes

As aforementioned, the variation in solar irradiance is one of the important reasons resulting in overvoltage. As such, different PV sizes should have different overvoltage risks. Using the proposed risk assessment method, a set of overvoltage risk profiles under different load levels in the 33-bus system versus different PV sizes are calculated and shown in Figure 5.6. It is noted that the maximum active power injections at different load levels are obtained from Table 5.2. The solar irradiance data in May, 2010 was used in the risk assessment with a Beta probability distribution shown in Figure 5.4.

Table 5.3 Maximum DG injection power at various load levels

Bus #	Pmax (kW) at various load levels					
	0.6	0.8	1	1.2	1.4	1.6
b1	500.00	500.00	500.00	500.00	500.00	500.00
b2	500.00	500.00	500.00	500.00	500.00	500.00
b3	500.00	500.00	500.00	500.00	500.00	500.00
b4	500.00	500.00	500.00	500.00	500.00	500.00
b5	500.00	500.00	500.00	500.00	500.00	500.00
b6	500.00	500.00	500.00	500.00	500.00	500.00
b7	500.00	500.00	500.00	500.00	500.00	500.00
b8	500.00	500.00	500.00	500.00	500.00	500.00
b9	302.50	500.00	500.00	500.00	500.00	500.00
b10	0.00	100.26	365.46	500.00	500.00	500.00
b11	0.00	0.01	0.00	165.28	467.69	500.00
b12	0.00	0.00	0.00	0.00	0.00	272.98
b13	0.00	0.00	0.00	0.00	0.00	0.00
b14	0.00	0.00	0.00	0.00	0.00	0.00
b15	0.00	0.00	0.00	0.00	0.00	0.01
b16	0.00	0.00	0.00	0.00	0.00	0.00
b17	0.00	0.00	0.00	0.00	0.00	0.00
b18	500.00	500.00	500.00	500.00	500.00	500.00
b19	500.00	500.00	500.00	500.00	500.00	500.00
b20	500.00	500.00	500.00	500.00	500.00	500.00
b21	500.00	500.00	500.00	500.00	500.00	500.00

b22	500.00	500.00	500.00	500.00	500.00	500.00
b23	500.00	500.00	500.00	500.00	500.00	500.00
b24	500.00	500.00	500.00	500.00	500.00	500.00
b25	500.00	500.00	500.00	500.00	500.00	500.00
b26	500.00	500.00	500.00	500.00	500.00	500.00
b27	500.00	500.00	500.00	500.00	500.00	500.00
b28	500.00	500.00	500.00	500.00	500.00	500.00
b29	207.88	500.00	500.00	500.00	500.00	500.00
b30	0.01	105.21	498.67	500.00	500.00	500.00
b31	0.00	0.01	0.00	360.70	500.00	500.00
b32	0.00	0.01	0.03	0.09	183.33	485.09
Tot.	10010.40	10705.51	11364.16	12026.07	12651.02	13258.09

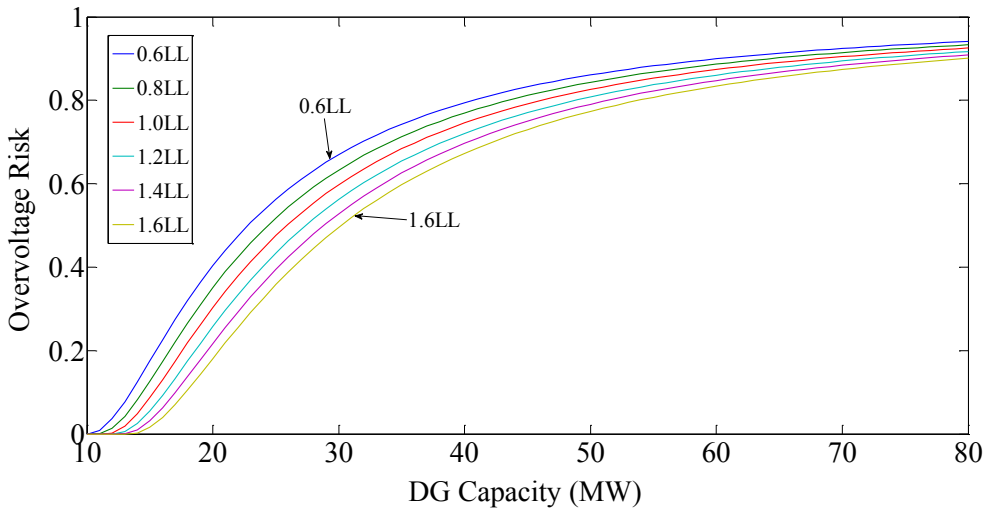

Figure 32 Risk analysis under different load levels.

It is obvious that the system will face higher overvoltage risks when more PVs are installed. The risk curve is somewhat like the cumulative probability distribution curve versus PV sizes. At the same time, it is observed that there is a higher risk when the system is in a low load condition. This observation is in accordance with the fact that overvoltage often happens under low load conditions.

Table 5.4 Bus voltage at various load levels

Bus #	Vbus (p.u.) at various load levels

	0.6	0.8	1	1.2	1.4	1.6
b0	1.0000	1.0000	1.0000	1.0000	1.0000	1.0000
b1	1.0039	1.0037	1.0034	1.0032	1.0030	1.0027
b2	1.0180	1.0172	1.0162	1.0152	1.0140	1.0127
b3	1.0259	1.0251	1.0241	1.0231	1.0218	1.0204
b4	1.0332	1.0326	1.0317	1.0308	1.0295	1.0280
b5	1.0451	1.0445	1.0434	1.0423	1.0405	1.0386
b6	1.0452	1.0444	1.0429	1.0415	1.0394	1.0371
b7	1.0482	1.0477	1.0465	1.0454	1.0438	1.0419
b8	1.0498	1.0500	1.0493	1.0489	1.0480	1.0469
b9	1.0486	1.0496	1.0496	1.0500	1.0499	1.0497
b10	1.0481	1.0491	1.0492	1.0499	1.0500	1.0500
b11	1.0473	1.0481	1.0479	1.0486	1.0492	1.0496
b12	1.0441	1.0438	1.0425	1.0422	1.0416	1.0433
b13	1.0429	1.0422	1.0405	1.0398	1.0388	1.0401
b14	1.0422	1.0412	1.0393	1.0383	1.0371	1.0381
b15	1.0414	1.0402	1.0381	1.0368	1.0354	1.0362
b16	1.0404	1.0388	1.0363	1.0347	1.0329	1.0333
b17	1.0400	1.0384	1.0357	1.0340	1.0321	1.0325
b18	1.0055	1.0052	1.0049	1.0046	1.0043	1.0039
b19	1.0172	1.0162	1.0152	1.0142	1.0132	1.0121
b20	1.0192	1.0181	1.0170	1.0159	1.0147	1.0135
b21	1.0210	1.0198	1.0186	1.0173	1.0160	1.0147
b22	1.0201	1.0186	1.0169	1.0152	1.0133	1.0114
b23	1.0218	1.0190	1.0160	1.0130	1.0099	1.0066
b24	1.0226	1.0192	1.0156	1.0120	1.0082	1.0043
b25	1.0467	1.0463	1.0453	1.0442	1.0425	1.0405
b26	1.0483	1.0480	1.0472	1.0463	1.0447	1.0427
b27	1.0498	1.0500	1.0496	1.0489	1.0472	1.0450
b28	1.0488	1.0495	1.0495	1.0490	1.0474	1.0451
b29	1.0476	1.0488	1.0494	1.0494	1.0481	1.0461
b30	1.0454	1.0465	1.0487	1.0500	1.0498	1.0489
b31	1.0449	1.0459	1.0479	1.0497	1.0500	1.0494
b32	1.0448	1.0457	1.0476	1.0494	1.0500	1.0500

5.5 Conclusion

This chapter presents a probabilistic method to evaluate the overvoltage risk due to high penetration of PVs in distribution networks. Based on V-P sensitivity analysis, an iterative algorithm has been developed to first calculate the maximum allowable active power injection from PVs without causing overvoltage problems. Secondly, the Kolmogorov–Smirnov test

(K–S test) was used to obtain the best distribution among a set of eight commonly used distributions for solar irradiance in different months in a year. Finally, the overvoltage risk is quantified for different PV capacity sizes under a given load level.

The effectiveness of proposed method has been verified on a 33-bus system. Simulation results show that the buses with lower V-P sensitivity have higher priority to install PVs. The allowable active injection is not only dependent on the V-P sensitivity but also affected by load levels. More PVs can be added into a distribution network when the system is more heavily loaded. For a given load level, the overvoltage risk increases when more PVs are placed in the system.

CHAPTER 6 SUMMARY AND FUTURE WORK

6.1 Summary

Voltage issues due to PV integration to distribution networks have to be carefully addressed before a high penetration of PV can be really achieved. A set of methods have been investigated in this work to accommodate high penetration of PV from the aspects of real time operation and control and combination with load management to the risk analysis and mitigation at the planning stage. More specifically, the following topics have been addressed:

In Chapter 2, we presented the impacts due to high penetration of PVs and PHEVs. More installation of PVs can lead to overvoltage while high penetration of PHEVs can cause undervoltage problems. It was shown by simulation in the chapter by using IEEE34 bus system.

Chapter 3 introduced a real power capping to control overvoltage over distribution networks with high penetration of PVs. The capping control provides control in real time over the inverters to keep voltage in the specified range with maximizing the PVs generation. The consensus control was used with capping control to make fairsharing in real power curtailments to show that distributed control can work as well. The advantage of this distributed method is to allow control of PVs without need of global information. The methods were verified by the simulation studies on a 33-bus system and IEEE 13 system.

Chapter 4 developed autonomous optimized schedules for controllable loads in three seasons which are winter, summer, and shoulder to minimize the energy cost for consumers. The schedules can be modified and utilized to accommodate PVs for residential customers who have PVs.

In Chapter 5, a probabilistic method was developed to evaluate the overvoltage risk due to high penetration of PVs in distribution networks. Based on V-P sensitivity analysis, an iterative algorithm has been developed to first calculate the maximum allowable active power injection from PVs without causing overvoltage problems. Secondly, the Kolmogorov–Smirnov test (K–S test) was used to obtain the best distribution among a set of eight commonly used distributions for solar irradiance in different months in a year. Finally, the overvoltage risk has been quantified for different PV capacity sizes under a given load level.

6.2 Future Work

The future research will still focus on 1) power source and load management to avoid overvoltage and undervoltage issues in distribution networks; and 2) Optimal sizing and placement of distributed photovoltaic sources to mitigate potential overvoltage issues due to high penetration of PVs.

6.2.1 Demand Side Management

Demand side management is another important aspect to alleviate overvoltage and undervoltage issues in high penetration distribution networks. The goal is to develop typical schedules for controllable residential loads without receiving command signals from utility companies [170], [171]. Based on the statistical analysis of the electricity cost and solar irradiance information for a specific location, a general management schedule have been developed for three types of loads and for the three different seasons during weekdays and weekends to achieve maximum likelihood of cost reduction while also reserving the load management resources to manage potential overvoltage issues due to high penetration of PVs.

In future work, the contribution plug-in hybrid electric vehicles (PHEVs) will be taken into account in demand side management. Meanwhile, we will propose a new optimal method in

coordination with the PV source control and demand side management methods. Monte Carlo simulation [172], [173] will be used to verify the effectiveness of proposed coordinate control method in consideration of different contingencies, load levels and system configurations.

6.2.2 PV Sizing and Placement

Improper location and sizing of PVs could lead to many negative effects on the distribution systems, such as the relay system configurations, voltage profiles, and power losses [174]. The placement of distributed PV sources in distribution network has great impact on the system power losses and voltage profiles. In general, the planning objectives can include: 1) maximization of PV penetration; 2) coordination with relay system in order to promise system reliability; 2) minimization of investment and operational cost 4) reduction system loss reduction while improving voltage profile.

Because the focus of this work is on voltage issues, the future research in PV sizing and placement will aim at minimizing the power loss while considering voltage profile. The following issues can be further investigated and explored

- The impact of adding PHEVs which are important energy storages in the near future, along with PVs installations on system losses.

REFERENCES

[1] Bloomberg. (2016). *The World Nears Peak Fossil Fuels for Electricity*. Available: http://www.bloomberg.com/news/articles/2016-06-13/we-ve-almost-reached-peak-fossil-fuels-for-electricity

[2] N. E. Institute. (2016). *History*. Available: http://www.nei.org

[3] U. S. E. I. Administration, "INTERNATIONAL ENERGY OUTLOOK 2016," 2016.

[4] U. S. E. I. Administration. (2016). *International Energy Outlook 2016*. Available: http://www.eia.gov/forecasts/ieo/pdf/0484(2016).pdf

[5] U. S. E. I. Adminstration. (2016). *Electricity*. Available: http://www.eia.gov/forecasts/ieo/pdf/electricity.pdf

[6] W. C. Association. (2016). *Coal and Electricity*. Available: http://www.worldcoal.org/coal/uses-coal/coal-electricity

[7] I. Dincer, "Renewable energy and sustainable development: a crucial review," *Renewable and Sustainable Energy Reviews,* vol. 4, pp. 157-175, 2000.

[8] H. Lund, "Renewable energy strategies for sustainable development," *Energy,* vol. 32, pp. 912-919, 2007.

[9] B. Commission, "Our common future: Report of the World Commission on Environment and Development," *UN Documents Gatheringa Body of Global Agreements,* 1987.

[10] B. D. Solomon and K. Krishna, "The coming sustainable energy transition: History, strategies, and outlook," *Energy Policy,* vol. 39, pp. 7422-7431, 2011.

[11] A. M. Omer, "Energy, environment and sustainable development," *Renewable and sustainable energy reviews,* vol. 12, pp. 2265-2300, 2008.

[12] K. Eisenack, "Institutional adaptation to cooling water scarcity for thermoelectric power generation under global warming," *Ecological Economics,* vol. 124, pp. 153-163, 2016.

[13] B. H. Hamududu and Å. Killingtveit, "Hydropower Production in Future Climate Scenarios: The Case for Kwanza River, Angola," *Energies,* vol. 9, p. 363, 2016.

[14] H. Haberl, M. Fischer-Kowalski, F. Krausmann, J. Martinez-Alier, and V. Winiwarter, "A socio-metabolic transition towards sustainability? Challenges for another Great Transformation," *Sustainable development,* vol. 19, pp. 1-14, 2011.

[15] P. Craig and G. De Búrca, *EU law: text, cases, and materials*: Oxford University Press, 2011.

[16] M. Labriet, S. R. Joshi, M. Vielle, P. B. Holden, N. R. Edwards, A. Kanudia*, et al.*, "Worldwide impacts of climate change on energy for heating and cooling," *Mitigation and Adaptation Strategies for Global Change,* vol. 20, pp. 1111-1136, 2015.

[17] S. Mima and P. Criqui, "Assessment of the impacts under future climate change on the energy systems with the POLES model," in *International energy workshop*, 2009.

[18] T. J. Wilbanks, P. Leiby, R. Perlack, J. T. Ensminger, and S. B. Wright, "Toward an integrated analysis of mitigation and adaptation: some preliminary findings," *Mitigation and Adaptation Strategies for Global Change,* vol. 12, pp. 713-725, 2007.

[19] COP21Paris. (2015). *COP - What's it all about?*

[20] S. Williams, "ohio'S CLEAN ENERGY FUTURE," 2015.

[21] M. Hand, T. Mai, S. Baldwin, G. Brinkman, D. Sandor, P. Denholm*, et al.*, "Renewable Electricity Futures Study-Volume One," National Renewable Energy Laboratory-Data

(NREL-DATA), Golden, CO (United States); National Renewable Energy Laboratory2016.

[22] T. N. Y. Times. (2016). *Inside the Paris Climate Deal*. Available: http://www.nytimes.com

[23] C. Zheng and D. M. Kammen, "An innovation-focused roadmap for a sustainable global photovoltaic industry," *Energy Policy,* vol. 67, pp. 159-169, 2014.

[24] M. A. Green, K. Emery, Y. Hishikawa, W. Warta, and E. D. Dunlop, "Solar cell efficiency tables (Version 45)," *Progress in photovoltaics: research and applications,* vol. 23, pp. 1-9, 2015.

[25] J. Jean, P. R. Brown, R. L. Jaffe, T. Buonassisi, and V. Bulović, "Pathways for solar photovoltaics," *Energy & Environmental Science,* vol. 8, pp. 1200-1219, 2015.

[26] N. R. Labaratory, "Efficiency Chart," 2015.

[27] J. Liang, J. Gong, J. Zhou, A. N. Ibrahim, and M. Li, "An open-source 3D solar radiation model integrated with a 3D Geographic Information System," *Environmental Modelling & Software,* vol. 64, pp. 94-101, 2015.

[28] C. Richter, S. Teske, and R. Short, *Global concentrating solar power outlook 09: Why Renewable energy is hot*: Greenpeace International, Solar Paces, Estela, 2009.

[29] N. S. Lewis and G. Crabtree, "Basic research needs for solar energy utilization: report of the basic energy sciences workshop on solar energy utilization, April 18-21, 2005," 2005.

[30] N. S. Lewis, "Research opportunities to advance solar energy utilization," *Science,* vol. 351, p. aad1920, 2016.

[31] L. a. g. intiative. (2015). *Total Surface Area Required to Fuel the World With Solar*.

[32] T. w. counts. (2014). *hese are hot topics these days...*

[33] U. E. P. Agency. (2012). *eGRID*.

[34] I. Fraunhofer, "Recent facts about photovoltaics in Germany," *Fraunhofer Institute for Solar Energy Systems, Germany, Tech. Rep.,[Online]. Available: http://www. abb-conversations. com/2014/01,* vol. 28, 2014.

[35] "China Targets 70 Gigawatts of Solar Power to Cut Coal Reliance," in *Bloomberg News* ed, 2014.

[36] (2015). *Snapshot of Global PV 1992-2014*.

[37] I. PVPS, "Snapshot of Global PV 1992-2014. Photovoltaic Power Systems Programme," *International Energy Agency,* 2015.

[38] M. McGranaghan, T. Ortmeyer, D. Crudele, T. Key, J. Smith, and P. Barker, "Renewable systems interconnection study: Advanced grid planning and operations," *Sandia National Laboratories,* 2008.

[39] N. Hiscock, T. G. Hazel, and J. Hiscock, "Voltage regulation at sites with distributed generation," *IEEE Transactions on industry applications,* vol. 44, pp. 445-454, 2008.

[40] T. T. Hashim, A. Mohamed, and H. Shareef, "A review on voltage control methods for active distribution networks," *Przeglad Elektrotechniczny (Electrical Review),* vol. 88, 2012.

[41] IEC, "Tap-Changers—Part 2: Application Guide," in *IEC Standard 60214-2*, ed, 2004.

[42] R. Tonkoski, L. A. Lopes, and T. H. El-Fouly, "Coordinated active power curtailment of grid connected PV inverters for overvoltage prevention," *IEEE Transactions on Sustainable Energy,* vol. 2, pp. 139-147, 2011.

[43] Y. Wang, P. Zhang, W. Li, W. Xiao, and A. Abdollahi, "Online overvoltage prevention control of photovoltaic generators in microgrids," *IEEE Transactions on Smart Grid,* vol. 3, pp. 2071-2078, 2012.

[44] R. Tonkoski and L. A. Lopes, "Voltage regulation in radial distribution feeders with high penetration of photovoltaic," in *Energy 2030 Conference, 2008. ENERGY 2008. IEEE*, 2008, pp. 1-7.

[45] J. Smith, W. Sunderman, R. Dugan, and B. Seal, "Smart inverter volt/var control functions for high penetration of PV on distribution systems," in *Power Systems Conference and Exposition (PSCE), 2011 IEEE/PES*, 2011, pp. 1-6.

[46] E. Demirok, D. Sera, R. Teodorescu, P. Rodriguez, and U. Borup, "Evaluation of the voltage support strategies for the low voltage grid connected PV generators," in *2010 IEEE Energy Conversion Congress and Exposition*, 2010, pp. 710-717.

[47] I. S. f. I. D. R. w. E. P. Systems, "IEEE Standard 1547-2003," ed, 2003.

[48] I. S. S. Development, "Development P1547a–Amendment 1 to IEEE Std 1547 ", ed, 2013.

[49] P. S. Georgilakis and N. D. Hatziargyrgio, "Optimal distributed generation placement in power distribution network," *IEEE Trans. on Power system,* vol. 28, pp. 3240-3248.

[50] A. Alarcon-Rodriguez, G. Ault, and S. Galloway, "Multi-objective planning of distributed energy resources: A review of the state-of-the-art," *Renewable and Sustainable Energy Reviews,* vol. 14, pp. 1353-1366, 2010.

[51] H. Yazdanpanahi, Y. W. Li, and W. Xu, "A new control strategy to mitigate the impact of inverter-based DGs on protection system," *IEEE Transactions on Smart Grid,* vol. 3, pp. 1427-1436, 2012.

[52] T. Saksornchai and B. Eua-arporn, "Determination of allowable capacity of distributed generation with protection coordination consideration," *Engineering Journal,* vol. 13, pp. 29-44, 2009.

[53] S. Favuzza, M. Ippolito, and F. Massaro, "Investigating the effect of distributed generators on traditional protection in radial distribution systems," in *PowerTech (POWERTECH), 2013 IEEE Grenoble*, 2013, pp. 1-6.

[54] E. Coster, J. Myrzik, and W. Kling, *Effect of DG on distribution grid protection*: INTECH Open Access Publisher, 2010.

[55] M. Matcha, S. K. Papani, and V. Killamsetti, "Adaptive relaying of radial distribution system with distributed generation," *International Journal of Electrical and Computer Engineering,* vol. 3, p. 407, 2013.

[56] J. Sadeh, M. Bashir, and E. Kamyab, "Effect of distributed generation capacity on the coordination of protection system of distribution network," in *Transmission and Distribution Conference and Exposition: Latin America (T&D-LA), 2010 IEEE/PES*, 2010, pp. 110-115.

[57] M. Alex and A. A. Josephine, "Impact due to the application location of a dispersed generation on the distribution system protection with SFCL application using PSCAD," in *Energy Efficient Technologies for Sustainability (ICEETS), 2013 International Conference on*, 2013, pp. 1225-1229.

[58] S. M. Brahma and A. A. Girgis, "Development of adaptive protection scheme for distribution systems with high penetration of distributed generation," *IEEE Transactions on Power Delivery,* vol. 19, pp. 56-63, 2004.

[59] V. R. Pandi, H. Zeineldin, and W. Xiao, "Determining optimal location and size of distributed generation resources considering harmonic and protection coordination limits," *IEEE Transactions on Power Systems,* vol. 28, pp. 1245-1254, 2013.

[60] S. Gonzalez, R. Bonn, and J. Ginn, "Removing barriers to utility interconnected photovoltaic inverters," in *Photovoltaic Specialists Conference, 2000. Conference Record of the Twenty-Eighth IEEE*, 2000, pp. 1691-1694.

[61] H. Zeineldin and J. L. Kirtley, "A simple technique for islanding detection with negligible nondetection zone," *IEEE Transactions on Power Delivery,* vol. 24, pp. 779-786, 2009.

[62] S. Syamsuddin, N. Rahim, and J. Selvaraj, "Implementation of TMS320F2812 in islanding detection for Photovoltaic Grid Connected Inverter," in *2009 International Conference for Technical Postgraduates (TECHPOS)*, 2009.

[63] I. PVPS, "Evaluation of islanding detection methods for photovoltaic utility-interactive power systems," *Report IEA PVPS T5-09,* 2002.

[64] A. Llaria, O. Curea, J. Jiménez, and H. Camblong, "Survey on microgrids: unplanned islanding and related inverter control techniques," *Renewable energy,* vol. 36, pp. 2052-2061, 2011.

[65] F. De Mango, M. Liserre, A. Dell'Aquila, and A. Pigazo, "Overview of anti-islanding algorithms for PV systems. Part I: Passive methods," in *Power Electronics and Motion Control Conference, 2006. EPE-PEMC 2006. 12th International*, 2006, pp. 1878-1883.

[66] S. J. Ranade, N. Prasad, S. Omick, and L. Kazda, "A study of islanding in utility-connected residential photovoltaic systems. I. models and analytical methods," *IEEE Transactions on Energy Conversion,* vol. 4, pp. 436-445, 1989.

[67] R. H. Wills, P. P. E. Engineer, and M. Harvard, *The interconnection of photovoltaic power systems with the utility grid: an overview for utility engineers*: Sandia National Laboratories, 1994.

[68] P. O'kane and B. Fox, "Loss of mains detection for embedded generation by system impedance monitoring," in *Developments in Power System Protection, Sixth International Conference on (Conf. Publ. No. 434)*, 1997, pp. 95-98.

[69] H. Mohamad, H. Mokhlis, and H. W. Ping, "A review on islanding operation and control for distribution network connected with small hydro power plant," *Renewable and Sustainable Energy Reviews,* vol. 15, pp. 3952-3962, 2011.

[70] G. Smith, P. Onions, and D. Infield, "Predicting islanding operation of grid connected PV inverters," *IEE Proceedings-Electric Power Applications,* vol. 147, pp. 1-6, 2000.

[71] B. Yu, M. Matsui, and G. Yu, "A review of current anti-islanding methods for photovoltaic power system," *Solar Energy,* vol. 84, pp. 745-754, 2010.

[72] T. Funabashi, K. Koyanagi, and R. Yokoyama, "A review of islanding detection methods for distributed resources," in *Power Tech Conference Proceedings*, 2003, pp. 1-6.

[73] J. H. Enslin, W. T. Hulshorst, A. M. Atmadji, P. J. Heskes, A. Kotsopoulos, J. Cobben, *et al.*, "Harmonic interaction between large numbers of photovoltaic inverters and the distribution network," in *Power Tech Conference Proceedings, 2003 IEEE Bologna*, 2003, p. 6 pp. Vol. 3.

[74] A. Chidurala, T. K. Saha, N. Mithulananthan, and R. C. Bansal, "Harmonic emissions in grid connected PV systems: a case study on a large scale rooftop PV site," in *2014 IEEE PES General Meeting| Conference & Exposition*, 2014, pp. 1-5.

[75] M. Kopicka, M. Ptacek, and P. Toman, "Analysis of the power quality and the impact of photovoltaic power plant operation on low-voltage distribution network," in *Electric Power Quality and Supply Reliability Conference (PQ), 2014*, 2014, pp. 99-102.

[76] W. Xu, "Status and future directions of power system harmonic analysis," *spectrum,* vol. 1, p. 1, 2004.

[77] M. Farhoodnea, A. Mohamed, H. Shareef, and H. Zayandehroodi, "An enhanced method for contribution assessment of utility and customer harmonic distortions in radial and weakly meshed distribution systems," *International Journal of Electrical Power & Energy Systems,* vol. 43, pp. 222-229, 2012.

[78] S. Osowski, "SVD technique for estimation of harmonic components in a power system: a statistical approach," *IEE Proceedings-Generation, Transmission and Distribution,* vol. 141, pp. 473-479, 1994.

[79] B. Swiatek, M. Rogoz, and Z. Hanzelka, "Power system harmonic estimation using neural networks," in *2007 9th International Conference on Electrical Power Quality and Utilisation*, 2007, pp. 1-8.

[80] P. K. Ray and B. Subudhi, "BFO optimized RLS algorithm for power system harmonics estimation," *Applied Soft Computing,* vol. 12, pp. 1965-1977, 2012.

[81] M. Świerczyński, R. Teodorescu, C. N. Rasmussen, P. Rodriguez, and H. Vikelgaard, "Overview of the energy storage systems for wind power integration enhancement," in *2010 IEEE International Symposium on Industrial Electronics*, 2010, pp. 3749-3756.

[82] S. Vazquez, S. Lukic, E. Galvan, L. G. Franquelo, J. M. Carrasco, and J. I. Leon, "Recent advances on energy storage systems," in *IECON 2011-37th Annual Conference on IEEE Industrial Electronics Society*, 2011, pp. 4636-4640.

[83] O. International. (2015). *Renewable energy in the United States*. Available: http://research.omicsgroup.org/index.php/Renewable_energy_in_the_United_States

[84] S. Bacha, D. Picault, B. Burger, I. Etxeberria-Otadui, and J. Martins, "Photovoltaics in microgrids: An overview of grid integration and energy management aspects," *Ieee Industrial Electronics Magazine,* vol. 9, pp. 33-46, 2015.

[85] C. Masters, "Voltage rise: the big issue when connecting embedded generation to long 11 kV overhead lines," *Power engineering journal,* vol. 16, pp. 5-12, 2002.

[86] N. Jenkins, *Embedded generation*: IET, 2000.

[87] "IEEE Recommended Practice for Utility Interface of Photovoltaic (PV) Systems, ," in *IEEE Std 929-2000.*, ed, 2000.

[88] A. F. Povlsen, "Impacts of power penetration from photovoltaic power systems in distribution networks," *Report IEA PVPS T5-10,* vol. 2002, 2002.

[89] Y. Ueda, K. Kurokawa, T. Tanabe, K. Kitamura, and H. Sugihara, "Analysis results of output power loss due to the grid voltage rise in grid-connected photovoltaic power generation systems," *IEEE Transactions on Industrial Electronics,* vol. 55, pp. 2744-2751, 2008.

[90] IEEE. *IEEE 34-node test system*. Available: http://ewh.ieee.org/soc/pes/dsacom/testfeeders/.

[91] I. P. a. E. Society. (2010). *Distribution Test Feeders*.

[92] H. Saadat, *Power System Analysis, McGraw Hill,* .

[93] W. Kempton and S. E. Letendre, "Electric vehicles as a new power source for electric utilities," *Transportation Research Part D: Transport and Environment,* vol. 2, pp. 157-175, 1997.

[94] C. Pang, P. Dutta, and M. Kezunovic, "BEVs/PHEVs as dispersed energy storage for V2B uses in the smart grid," *IEEE Transactions on Smart Grid,* vol. 3, pp. 473-482, 2012.

[95] N. Rotering and M. Ilic, "Optimal charge control of plug-in hybrid electric vehicles in deregulated electricity markets," *IEEE Transactions on Power Systems,* vol. 26, pp. 1021-1029, 2011.

[96] S. Deilami, A. S. Masoum, P. S. Moses, and M. A. Masoum, "Real-time coordination of plug-in electric vehicle charging in smart grids to minimize power losses and improve voltage profile," *Smart Grid, IEEE Transactions on,* vol. 2, pp. 456-467, 2011.

[97] K. Clement-Nyns, E. Haesen, and J. Driesen, "The impact of charging plug-in hybrid electric vehicles on a residential distribution grid," *Power Systems, IEEE Transactions on,* vol. 25, pp. 371-380, 2010.

[98] S. J. Moura, H. K. Fathy, D. S. Callaway, and J. L. Stein, "A stochastic optimal control approach for power management in plug-in hybrid electric vehicles," *Control Systems Technology, IEEE Transactions on,* vol. 19, pp. 545-555, 2011.

[99] S. Shao, M. Pipattanasomporn, and S. Rahman, "Demand response as a load shaping tool in an intelligent grid with electric vehicles," *Smart Grid, IEEE Transactions on,* vol. 2, pp. 624-631, 2011.

[100] A. S. Masoum, S. Deilami, P. S. Moses, M. Masoum, and A. Abu-Siada, "Smart load management of plug-in electric vehicles in distribution and residential networks with charging stations for peak shaving and loss minimisation considering voltage regulation," *Generation, Transmission & Distribution, IET,* vol. 5, pp. 877-888, 2011.

[101] M. Pipattanasomporn, M. Kuzlu, and S. Rahman, "An algorithm for intelligent home energy management and demand response analysis," *Smart Grid, IEEE Transactions on,* vol. 3, pp. 2166-2173, 2012.

[102] P. Du and N. Lu, "Appliance commitment for household load scheduling," *Smart Grid, IEEE Transactions on,* vol. 2, pp. 411-419, 2011.

[103] A. Molderink, V. Bakker, M. G. Bosman, J. L. Hurink, and G. J. Smit, "Management and control of domestic smart grid technology," *Smart grid, IEEE transactions on,* vol. 1, pp. 109-119, 2010.

[104] N. Ruiz, I. Cobelo, and J. Oyarzabal, "A direct load control model for virtual power plant management," *Power Systems, IEEE Transactions on,* vol. 24, pp. 959-966, 2009.

[105] M. Thomson and D. G. Infield, "Network power-flow analysis for a high penetration of distributed generation," *Power Systems, IEEE Transactions on,* vol. 22, pp. 1157-1162, 2007.

[106] E. J. Coster, J. M. Myrzik, B. Kruimer, and W. L. Kling, "Integration issues of distributed generation in distribution grids," *Proceedings of the IEEE,* vol. 99, pp. 28-39, 2011.

[107] C.-S. Chen, C.-H. Lin, W.-L. Hsieh, C.-T. Hsu, T.-T. Ku, and C.-Y. Ho, "Effect of load transfer to penetration level of PV generation in distribution system," in *Innovative Smart Grid Technologies-Asia (ISGT Asia), 2012 IEEE*, 2012, pp. 1-6.

[108] C.-H. Lin, W.-L. Hsieh, C.-S. Chen, C.-T. Hsu, T.-T. Ku, and C.-T. Tsai, "Financial analysis of a large-scale photovoltaic system and its impact on distribution feeders," *Industry Applications, IEEE Transactions on,* vol. 47, pp. 1884-1891, 2011.

[109] Y. Wang, P. Zhang, W. Li, W. Xiao, and A. Abdollahi, "Online Overvoltage Prevention Control of Photovoltaic Generators in Microgrids," *Smart Grid, IEEE Transactions on* vol. 3, pp. 2071 - 2078, 2012.

[110] R. Tonkoski, L. A. Lopes, and T. H. El-Fouly, "Coordinated active power curtailment of grid connected PV inverters for overvoltage prevention," *Sustainable Energy, IEEE Transactions on,* vol. 2, pp. 139-147, 2011.

[111] T. Hazel, N. Hiscock, and J. Hiscock, "Voltage regulation at sites with distributed generation," *Industry Applications, IEEE Transactions on,* vol. 44, pp. 445-454, 2008.

[112] T. J. T. Hashim, A. Mohamed, and H. Shareef, "A review on voltage control methods for active distribution networks," *PRZEGLAD ELEKTROTECHNICZNY,* vol. 88, pp. 304-312, 2012.

[113] IEC, "Tap-changers - Part 2: Application Guide " in *IEC Std. 60214-2*, ed, 2004.

[114] E. Demirok, D. Sera, R. Teodorescu, P. Rodriguez, and U. Borup, "Evaluation of the voltage support strategies for the low voltage grid connected PV generators," in *Energy Conversion Congress and Exposition (ECCE), 2010 IEEE*, 2010, pp. 710-717.

[115] I. Std, "IEEE Standard for Interconnecting Distributed Resources with Electric Power Systems. ," in *IEEE Std 1547TM-2003,* , ed, 2003.

[116] M. Alam, K. Muttaqi, and D. Sutanto, "Mitigation of Rooftop Solar PV Impacts and Evening Peak Support by Managing Available Capacity of Distributed Energy Storage Systems," *IEEE Trans Power Syst,* 2013.

[117] H. Ayres, W. Freitas, M. De Almeida, and L. Da Silva, "Method for determining the maximum allowable penetration level of distributed generation without steady-state voltage violations," *IET generation, transmission & distribution,* vol. 4, pp. 495-508, 2010.

[118] L. Yu, D. Czarkowski, and F. De Leon, "Optimal distributed voltage regulation for secondary networks with DGs," *IEEE Transactions on Smart Grid,* vol. 3, pp. 959-967, 2012.

[119] P. Tenti, H. K. M. Paredes, and P. Mattavelli, "Conservative Power Theory, a Framework to Approach Control and Accountability Issues in Smart Microgrids," *IEEE Transactions on Power Electronics,* vol. 26, pp. 664-73, 03/ 2011.

[120] H. Xin, Z. Qu, J. Seuss, and A. Maknouninejad, "A self-organizing strategy for power flow control of photovoltaic generators in a distribution network," *IEEE Transactions on Power Systems,* vol. 26, pp. 1462-1473, 2011.

[121] IEEE, "IEEE Recommended Practice for Utility Interface of Photovoltaic (PV) Systems," in *IEEE Std 929-2000*, ed, 2000.

[122] IEEE, "IEEE Application Guide for IEEE Std 1547, IEEE Standard for Interconnecting Distributed Resources with Electric Power Systems," in *Std 1547.2-2008*, ed, 2009.

[123] CSA, "CAN/CSA C22.2 NO. 257-06 (R2011) - Interconnecting Inverter-based Micro-distributed Resources to Distribution Systems," ed, 2006.

[124] CSA, "CAN3 C235-83 (R2006), Preferred Voltage Levels for AC Systems, 0 to 50 000 V," ed, 2006.

[125] L. Y. Wang, C. Wang, G. Yin, and Y. Wang, "Weighted and constrained consensus for distributed power flow control," presented at the PMAPS 2012, Istanbul, Turkey, 2012.

[126] G. Yin, Y. Sun, and L. Y. Wang, "Asymptotic properties of consensus-type algorithms for networked systems with regime-switching topologies," *Automatica,* vol. 47, pp. 1366-1378, 2011.

[127] G. Chen and F. L. Lewis, "Distributed tracking control for networked mechanical systems," *Asian Journal of Control,* vol. 14, pp. 1459-1469, 2012.

[128] H. Minyi and J. H. Manton, "Coordination and consensus of networked agents with noisy measurements: stochastic algorithms and asymptotic behavior," *SIAM Journal on Control and Optimization,* vol. 48, pp. 131-58, / 2009.

[129] R. Wei and R. W. Beard, "Consensus seeking in multiagent systems under dynamically changing interaction topologies," *IEEE Transactions on Automatic Control,* vol. 50, pp. 655-61, 05/ 2005.

[130] M. E. Baran and F. F. Wu, "Network reconfiguration in distribution systems for loss reduction and load balancing," *IEEE Transactions on Power Delivery,* vol. 4, pp. 1401-1407, 1989.

[131] W. Kersting, "Radial distribution test feeders," in *2001 IEEE Power Engineering Society Winter Meeting, January 28, 2001 - February 1, 2001*, Columbus, OH, United states, 2001, pp. 908-912.

[132] MathWorks. (2013). *SimPowerSystems User's Guide*. Available: http://www.mathworks.com/help/pdf_doc/physmod/powersys/powersys.pdf

[133] C. Wang and M. H. Nehrir, "Power management of a stand-alone wind/photovoltaic/fuel cell energy system," *IEEE transactions on energy conversion,* vol. 23, pp. 957-967, 2008.

[134] W. H. Kersting, "Radial distribution test feeders," in *Power Engineering Society Winter Meeting, 2001. IEEE*, 2001, pp. 908-912.

[135] J. Zhao, C. Wang, B. Zhao, F. Lin, Q. Zhou, and Y. Wang, "A review of active management for distribution networks: current status and future development trends," *Electric Power Components and Systems,* vol. 42, pp. 280-293, 2014.

[136] D. Kothari, "Power system optimization," in *Computational Intelligence and Signal Processing (CISP), 2012 2nd National Conference on*, 2012, pp. 18-21.

[137] C. Wang, C. J. Miller, M. H. Nehrir, J. W. Sheppard, and S. P. McElmurry, "A load profile management integrated power dispatch using a Newton-like particle swarm optimization method," *Sustainable Computing: Informatics and Systems,* 2014.

[138] P. Jazayeri, A. Schellenberg, W. Rosehart, J. Doudna, S. Widergren, D. Lawrence*, et al.*, "A survey of load control programs for price and system stability," *Power Systems, IEEE Transactions on,* vol. 20, pp. 1504-1509, 2005.

[139] D. M. Laverty, D. J. Morrow, R. Best, and P. A. Crossley, "Telecommunications for smart grid: Backhaul solutions for the distribution network," in *Power and Energy Society General Meeting, 2010 IEEE*, 2010, pp. 1-6.

[140] A.-H. Mohsenian-Rad, V. W. Wong, J. Jatskevich, R. Schober, and A. Leon-Garcia, "Autonomous demand-side management based on game-theoretic energy consumption scheduling for the future smart grid," *Smart Grid, IEEE Transactions on,* vol. 1, pp. 320-331, 2010.

[141] G. T. Costanzo, G. Zhu, M. F. Anjos, and G. Savard, "A system architecture for autonomous demand side load management in smart buildings," *Smart Grid, IEEE Transactions on,* vol. 3, pp. 2157-2165, 2012.

[142] K. Herter, "Residential implementation of critical-peak pricing of electricity," *Energy Policy,* vol. 35, pp. 2121-2130, 2007.

[143] M. M. Rogers, G. Xu, C. J. Miller, S. P. McElmurry, W. Shi, Y. Wang, *et al.*, "HERO: A smart-phone application for location based emissions estimates," *Sustainable Computing: Informatics and Systems,* 2014.

[144] R. Tonkoski, D. Turcotte, and T. H. El-Fouly, "Impact of high PV penetration on voltage profiles in residential neighborhoods," *Sustainable Energy, IEEE Transactions on,* vol. 3, pp. 518-527, 2012.

[145] S. Alyami, Y. Wang, C. Wang, J. Zhao, and B. Zhao, "Adaptive real power capping method for fair overvoltage regulation of distribution networks with high penetration of pv systems," 2014.

[146] MISO, "Historical LMP," ed, 2013.

[147] National Renewable Laboratory. (2010). *National Solar Radiation Data Base 2010* Available: http://rredc.nrel.gov/solar/old_data/nsrdb/1991-2010/hourly/siteonthefly.cgi?id=725416

[148] (2013). *IEEE SCC21 1547 Standards Development P1547a–Amendment 1 to IEEE Std 1547 Working Group Meeting Minutes for June 13–14, 2013*. Available: http://grouper.ieee.org/

[149] H. M. Ayres, W. Freitas, M. C. de Almeida, and L. C. da Silva, "Method for determining the maximum allowable penetration level of distributed generation without steady-state voltage violations," *Generation, Transmission & Distribution, IET,* vol. 4, pp. 495-508, 2010.

[150] L. Yu, D. Czarkowski, and F. De León, "Optimal distributed voltage regulation for secondary networks with DGs," *Smart Grid, IEEE Transactions on,* vol. 3, pp. 959-967, 2012.

[151] Y. Wang, P. Zhang, W. Li, W. Xiao, and A. Abdollahi, "Online overvoltage prevention control of photovoltaic generators in microgrids," *Smart Grid, IEEE Transactions on,* vol. 3, pp. 2071-2078, 2012.

[152] S. Alyami, Y. Wang, C. Wang, J. Zhao, and B. Zhao, "Adaptive real power capping method for fair overvoltage regulation of distribution networks with high penetration of PV systems," *Smart Grid, IEEE Transactions on,* vol. 5, pp. 2729-2738, 2014.

[153] P. S. Georgilakis and N. D. Hatziargyriou, "Optimal distributed generation placement in power distribution networks: models, methods, and future research," *IEEE Transactions on Power Systems,* vol. 28, pp. 3420-3428, 2013.

[154] M. F. Shaaban, Y. M. Atwa, and E. F. El-Saadany, "DG allocation for benefit maximization in distribution networks," *Power Systems, IEEE Transactions on,* vol. 28, pp. 639-649, 2013.

[155] W. El-Khattam, Y. Hegazy, and M. Salama, "An integrated distributed generation optimization model for distribution system planning," *Power Systems, IEEE Transactions on,* vol. 20, pp. 1158-1165, 2005.

[156] K. Nekooei, M. M. Farsangi, H. Nezamabadi-Pour, and K. Y. Lee, "An improved multi-objective harmony search for optimal placement of DGs in distribution systems," *Smart Grid, IEEE Transactions on,* vol. 4, pp. 557-567, 2013.

[157] C. L. Borges and D. M. Falcao, "Optimal distributed generation allocation for reliability, losses, and voltage improvement," *International Journal of Electrical Power & Energy Systems,* vol. 28, pp. 413-420, 2006.

[158] A. Kudish and A. Ianetz, "Analysis of daily clearness index, global and beam radiation for Beer Sheva, Israel: Partition according to day type and statistical analysis," *Energy Conversion and Management,* vol. 37, pp. 405-416, 1996.

[159] T. P. Chang, "Investigation on frequency distribution of global radiation using different probability density functions," *International Journal of Applied Science and Engineering 8 (2),* pp. 99-107, 2010.

[160] K. G. T. Hollands and R. Huget, "A probability density function for the clearness index, with applications," *Solar Energy,* vol. 30, pp. 195-209, 1983.

[161] H. Assuncao, J. Escobedo, and A. Oliveira, "A new algorithm to estimate sky condition based on 5 minutes-averaged values of clearness index and relative optical air mass," *Theoretical and Applied Climatology,* vol. 90, pp. 235-248, 2007.

[162] Y. D. Arthur, K. B. Gyamfi, and S. Appiah, "Probability distributional analysis of hourly solar irradiation in Kumasi-Ghana," *International Journal of Business and Social Research,* vol. 3, pp. 63-75, 2013.

[163] A. Abdulkarim, S. M. Abdelkader, and D. J. Morrow, "Statistical Analyses of Wind and Solar Energy Resources for the Development of Hybrid Microgrid," in *2nd*

International Congress on Energy Efficiency and Energy Related Materials (ENEFM2014), 2015, pp. 9-14.

[164] V. L. Brano, A. Orioli, G. Ciulla, and S. Culotta, "Quality of wind speed fitting distributions for the urban area of Palermo, Italy," *Renewable Energy,* vol. 36, pp. 1026-1039, 2011.

[165] X.-F. Wang, Y. Song, and M. Irving, *Modern power systems analysis*: Springer Science & Business Media, 2010.

[166] (2010). *National Solar Radiation Data Base* Available: http://www.nrel.gov/rredc/

[167] M. Liu, W. Li, R. Billinton, C. Wang, and J. Yu, "Modeling tidal current speed using a Wakeby distribution," *Electric Power Systems Research,* vol. 127, pp. 240-248, 2015.

[168] J. Wang, W. W. Tsang, and G. Marsaglia, "Evaluating Kolmogorov's distribution," *Journal of Statistical Software,* vol. 8, 2003.

[169] K. Nekooei, M. M. Farsangi, H. Nezamabadi-Pour, and K. Y. Lee, "An improved multi-objective harmony search for optimal placement of DGs in distribution systems," *IEEE Transactions on smart grid,* vol. 4, pp. 557-567, 2013.

[170] W.-Y. Chiu, H. Sun, and H. V. Poor, "Energy imbalance management using a robust pricing scheme," *IEEE Transactions on Smart Grid,* vol. 4, pp. 896-904, 2013.

[171] G. o. W. Australia, "Demand Side Management," ed, 2010.

[172] D. H. McQueen, P. R. Hyland, and S. J. Watson, "Monte Carlo simulation of residential electricity demand for forecasting maximum demand on distribution networks," *IEEE Transactions on power systems,* vol. 19, pp. 1685-1689, 2004.

[173] I. Richardson, M. Thomson, and D. Infield, "A high-resolution domestic building occupancy model for energy demand simulations," *Energy and buildings,* vol. 40, pp. 1560-1566, 2008.

[174] P. Paliwal, N. Patidar, and R. Nema, "Planning of grid integrated distributed generators: A review of technology, objectives and techniques," *Renewable and Sustainable Energy Reviews,* vol. 40, pp. 557-570, 2014.

ABSTRACT

VOLTAGE MANAGEMENT OF DISTRIBUTION NETWORKS WITH HIGH PENETRATION OF DISTRIBUTED PHOTOVOLTAIC GENERATION SOURCES

by

SAEED ALYAMI

August 2016

Advisor: Professor Caisheng Wang

Major: Electrical and Computer Engineering

Degree: Doctor of Philosophy

Installation of photovoltaic (PV) units could lead to great challenges to the existing electrical systems. Issues such as voltage rise, protection coordination, islanding detection, harmonics, increased or changed short-circuit levels, etc., need to be carefully addressed before we can see a wide adoption of this environmentally friendly technology. Voltage rise or overvoltage issues are of particular importance to be addressed for deploying more PV systems to distribution networks. This research proposes a comprehensive solution to deal with the voltage violations in distribution networks, from controlling PV power outputs and electricity consumption of smart appliances in real time to optimal placement of PVs at the planning stage. A new real power capping method is investigated to prevent overvoltage by adaptively setting the power caps for PV inverters in real time. The proposed method can maintain voltage profiles below a pre-set upper limit while maximizing the PV generation and fairly distributing the real power curtailments among all the PV systems in the network. As a result, each of the PV systems in the network has equal opportunity to generate electricity and shares the

responsibility of voltage regulation. The method does not require global information and can be implemented either under a centralized supervisory control scheme or in a distributed way via consensus control. Furthermore, the research investigates autonomous operation schedules for three types of intelligent appliances (or residential controllable loads) without receiving external signals for cost saving and for assisting the management of possible photovoltaic generation systems installed in the same distribution network. The three types of controllable loads studied in the chapter are electric water heaters, refrigerators deicing loads, and dishwashers, respectively. Also, the study explores the method to mitigate overvoltage issues at the planning stage. A probabilistic method is introduced to evaluate the overvoltage risk in a distribution network with different PV capacity sizes under different load levels. Kolmogorov–Smirnov test (K–S test) is used to identify the most proper probability distributions for solar irradiance in different months. To increase accuracy, an iterative process is used to obtain the maximum allowable injection of active power from PVs.

AUTOBIOGRAPHICAL STATEMENT

SAEED ALYAMI

Education

2016 Doctor of Philosophy, Wayne State University, Detroit, MI, USA
2011 Master Degree in Electrical Engineering, Wayne State University, Detroit, MI, USA
2004 Bachelor Degree in Electrical Engineering, King Fahd University of Petroleum and Minerals, Dhahran, Saudi Arabia

Journal

1. S. Alyami, Y. Wang, C. Wang, J. Zhao, and B. Zhao, "Adaptive real power capping method for fair overvoltage regulation of distribution networks with high penetration of PV systems," *IEEE Transactions on Smart Grid,* vol. 5, pp. 2729-2738, 2014.

Conference

1. S. Alyami, C. Wang, and C. Fu, "Development of autonomous schedules of controllable loads for cost reduction and PV accommodation in residential distribution networks," in *Electrical Power and Energy Conference (EPEC), 2015 IEEE*, 2015, pp. 81-86.
2. S. Alyami, Y. Wang, C. Wang, "Overvoltage Risk Analysis in Distribution Networks with High Penetration of PVs" 2016 International Conference on Probabilistic Methods Applied to Power Systems, (Accepted)